Tetra- and Octalactam Macrocycles and Catenanes with Exocyclic Metal Coordination Sites: Versatile Building Blocks for Supramolecular Chemistry

Xi-you Li,[a] Jens Illigen,[a] Martin Nieger,[b] Steffen Michel,[a] and Christoph A. Schalley*[a]

Abstract: The synthesis of a new tetralactam macrocycle and the simultaneous formation of catenanes and larger octalactam macrocycles is reported. These species bear 2,2′-biquinoline moieties suitably positioned to bind a metal center at the outer periphery of the macrocycles. ^{1}H NMR chemical shifts permit the unambiguous distinction of transoid and cisoid conformations of the biquinoline moiety, thereby allowing an unequivocal identification of the catenane and octalactam structures, despite the fact that both have the same elemental composition and bear identical structural subunits. With the aid of an anion template effect, rotaxanes can be prepared from the smaller tetralactam macrocycle. These reveal significantly altered requirements in terms of the stopper size as compared to previously reported tetralactam wheels. Several copper(I)-mediated dimers and a $(bpy)_2Ru^{II}$ complex (bpy = 2,2′-bipyridine) have been synthesized from the tetralactam macrocycle and the rotaxanes. The anion binding abilities of the tetralactam macrocycle and its $(bpy)_2Ru^{II}$ complex in DMSO have been compared by ^{1}H NMR titration experiments, which revealed significantly enhanced binding by the metal complex. Mass spectrometry has been used to study the potential formation of larger assemblies of copper(I) and the catenane built-up from two tetralactam macrocycles. Indeed, a 2:2 complex was identified. In contrast, the octalactam macrocycle of the same elemental composition yields only 1:1 complexes, with the Cu^I ion connecting its two biquinoline moieties in the center of a figure-eight-shaped molecule. Molecular modeling studies support the structural assignments made.

Keywords: supramolecular chemistry · rotaxanes · catenanes · anion receptors · self-assembly

Introduction

Rotaxanes, that is axles threaded through macrocycles equipped with two stopper groups to prevent dethreading, and catenanes,[1] that is two interlocking macrocycles, can now be efficiently assembled with the aid of several different template effects.[2] There exist a variety of approaches, including those based on the tetrahedral[3] or octahedral[4] coordination geometry of metal ions, π-donor/π-acceptor interactions,[5] and hydrogen bonding involving ammonium ions,[6] neutral amides,[7] or phenolate stoppers.[8] With these methods at hand, the research in this field has become increasingly focused on the properties of the mechanical bond, among them topological chirality,[9] electron- or energy transfer from one stopper to the other,[10] the quenching of luminescence in self-assembled pseudorotaxanes,[11] the photoswitchability of the catenanes' ring geometry,[12] electrical conductance through polyrotaxanes,[13] and the kinetics of the deslipping reaction which liberates the wheel and axle without cleavage of a covalent bond.[14] Two of the most intriguing applications of rotaxanes are the construction of logic gates[15] and rotary devices[16] at the molecular level.

Herein, we report the synthesis of new tetralactam and octalactam macrocycles bearing one or two biquinoline moieties, respectively, that allow the binding of metal centers to their outer periphery. Catenanes are also formed in the macrocyclization step, which can be distinguished from the octalactam macrocycles of identical elemental composition by ^{1}H NMR experiments. The smaller macrocycle can be utilized for the synthesis of rotaxanes. Several Cu^I complexes of these species have been prepared. The complexes of Cu^I are of particular interest, because previous examples have shown their ability to effect the catalytic reduction of dioxygen,[17] their diverse activities in many biological systems,[18] and their ability to transfer energy to anthracene, which may prove useful in photocatalytic solar energy harvesting systems.[19]

[a] Dr. C. A. Schalley, Dr. X.-y. Li,[+] J. Illigen, S. Michel
Kekulé-Institut für Organische Chemie und Biochemie
Universität Bonn
Gerhard-Domagk-Strasse 1, 53121 Bonn (Germany)
Fax: (+49) 228-735662
E-mail: c.schalley@uni-bonn.de

[b] Dr. M. Nieger
Institut für Anorganische Chemie, Universität Bonn
Gerhard-Domagk-Strasse 1, 53121 Bonn (Germany)

[+] Present address: Shandong Normal University, Ji Nan, 250014 (China)

  0947-6539/03/0906-1332 $ 20.00+.50/0

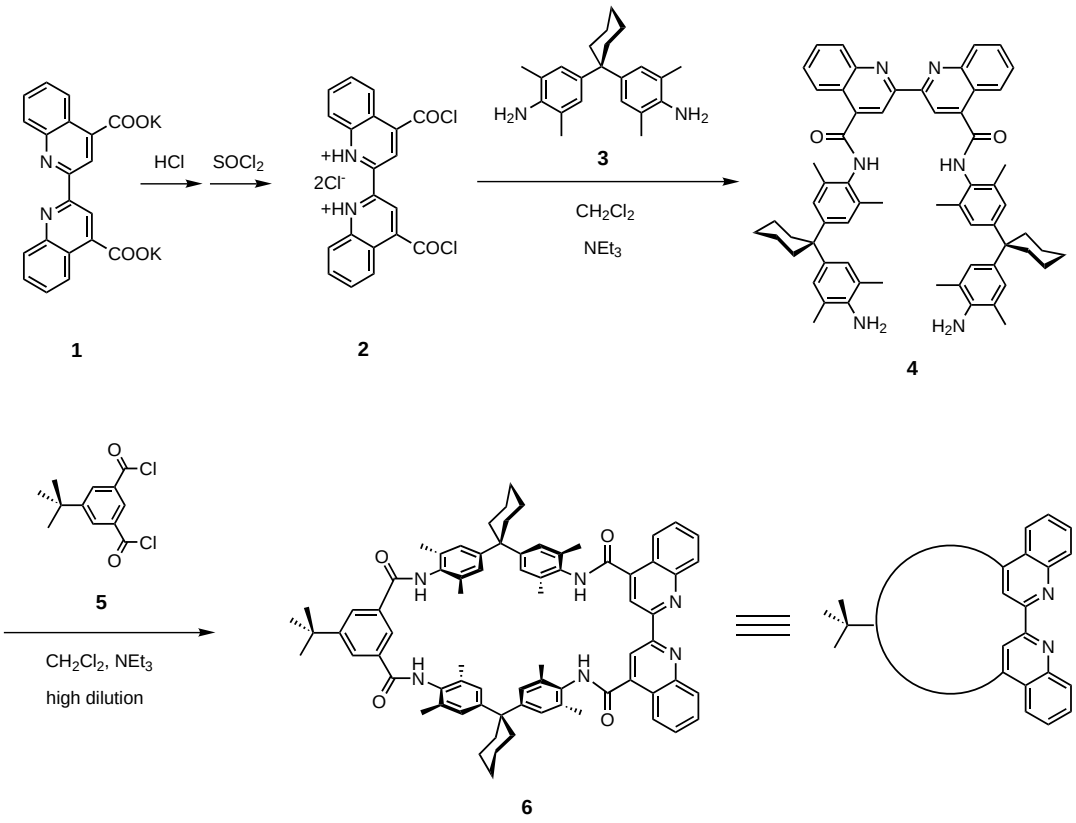

Scheme 1. Synthesis of **6**.

Abstract in German: *Die Synthese eines neuen Tetralactam-Macrocyclus und die gleichzeitige Bildung von Catenanen und größeren Octalactam-Cyclen wird beschrieben. Diese Moleküle enthalten 2,2′-Bischinolin-Einheiten in einer Position, die die Bindung von Metallkationen an der Außenseite des Macrocyclus erlaubt. ^{1}H-NMR-chemische Verschiebungen gestatten die eindeutige Zuordnung der transoiden bzw. cisoiden Konformationen der Bischinolin-Einheit und ermöglichen damit eine sichere Identifikation von Catenanen und Octalactam-Cyclus, obwohl beide dieselbe Elementarzusammensetzung haben und identische strukturelle Untereinheiten enthalten. Mittels eines Anionentemplateffekts können Rotaxane des kleineren Tetralactam-Reifs synthetisiert werden, der gegenüber früheren Tetralactam-Cyclen deutlich veränderte Größenanforderungen an den Stopper stellt. Kupfer(*i*)-verbrückte Dimere und ein (bpy)$_2$Ru(*ii*)-Komplex des Tetralactam-Macrocyclus und der Rotaxane wurden synthetisiert. Die Anionenbindungsfähigkeit des Tetralactam-Cyclus in DMSO wurde mit seinem (bpy)$_2$Ru^{II}-Gegenstück verglichen und ^{1}H-NMR-Titrationsexperimente zeigen eine deutlich verstärkte Anionenbindung an den Metallkomplex. Die Massenspektrometrie eignet sich für die Detektion größerer Komplexe von Kupfer(*i*)-Ionen mit dem Catenan aus zwei Tetralactam-Reifen. Tatsächlich bildet sich ein 2:2-Komplex. Hingegen bildet der Octalactam-Macrocyclus gleicher Zusammensetzung lediglich 1:1-Komplexe, in denen ein Cu^I-Ion die beiden Bischinolin-Untereinheiten im Zentrum eines achtförmigen Moleküls verbindet. Molecular Modeling unterstützt die strukturellen Aussagen.*

Also, the (bpy)$_2$Ru^{II} complex (bpy = 2,2′-bipyridine) of the tetralactam macrocycle has been synthesized and its anion binding properties[20] have been examined in comparison to those of the tetralactam macrocycle alone.

Another aspect attracting considerable recent interest is that of the self-assembly of structures of nanometer dimensions from simpler building blocks.[21] Utilizing the tetrahedral coordination geometry of copper(i) ions, many different types of assemblies have been reported, prominent examples being the grid-type complexes[22] of Lehn and others and the copper-templated rotaxanes and catenanes mentioned above.[3] Both the catenane made from two tetralactam wheels and the octalactam macrocycle bear two metal coordination sites and could therefore be expected to yield larger assemblies on addition of copper ions. This aspect has been studied using ESI mass spectrometry.

Results and Discussion

Synthesis of macrocycles and catenanes

The synthesis of the tetralactam macrocycle is shown in Scheme 1. The biquinoline dicarboxylic acid salt **1** is first converted to the acid chloride **2** and then coupled with diamine **3** to yield building block **4** according to well-known literature procedures.[23] A macrocyclization with acid chloride **5** carried out under high dilution conditions yields the desired macrocycle **6** in a disappointingly low yield of only about 10%. In fact, three additional products could be separated: a catenane **7** built from two interlocked wheels **6** in

  0947-6539/03/0906-1333 $ 20.00+.50/0

1% yield, a larger octalactam macrocycle **8** as the major product (32%), and, presumably, a catenane **9** assembled from one octalactam and one tetralactam wheel (7%). However, catenane **9** could not be fully characterized due to its complicated NMR spectra (see Experimental Section). All attempts to increase the yield of **6** by optimizing this route, for example by further decreasing the concentration of the reactants in order to shift the ratio of the two macrocycles towards **6**, were unsuccessful. Starting with the acid chloride **5** in the first reaction with **3** and subsequent macrocyclization with **2** did not give higher yields either.

Single-crystal X-ray structural data (Table 1) and results from molecular modeling (Figure 1) on intermediate **4** suggest that the biquinoline moiety exists primarily in a transoid conformation. In this conformation, unfavorable interactions between the lone pairs located on the biquinoline nitrogen atoms, as well as between the hydrogen atoms in the 3- and 3′-positions, are avoided. The π system is almost planar, thus maximizing delocalization. Figure 1 (top) shows a superposition of the 40 most favorable conformers found in a 3000 step Monte Carlo conformational search performed with the Amber* force field[24] as implemented in MacroModel 7.0.[25] In all of these structures, which lie within a range of about 5 kcal mol^{-1} above the lowest-energy structure, the central biquinoline part is transoid, while the amide groups appear to have four different favorable positions (carbonyl groups above or below the ring plane and pointing outwards or inwards). Furthermore, the diamine arms are rather rigid, but can be rotated about the amide – benzene single bonds, so that they show several different orientations with respect to the biquinoline plane that are similar in energy. Single crystals of **4** suitable for X-ray structure analysis were obtained by recrystallization from DMSO. In the crystal structure, the central biquinoline part of this building block is again seen to be in a transoid conformation, confirming the results obtained from modeling. The side arms are, however, more or less fixed, probably due to packing effects. Several hydrogen bonds are formed, either to neighboring molecules or to DMSO molecules in the crystal.[26]

Table 1. Crystallographic data and summary of data collection and refinement for **4**.

formula	$C_{64}H_{68}N_6O_2 \cdot 7\,C_2H_6OS$
crystal system	triclinic
space group	$P\bar{1}$ (no. 2)
a [Å]	7.6535(2)
b [Å]	22.3356(5)
c [Å]	25.6017(7)
α [°]	107.769(1)
β [°]	96.686(1)
γ [°]	96.780(1)
V [Å^3]	4087.2(2)
Z	2
ρ [g cm^{-3}]	1.22
μ [mm^{-1}]	0.250
diffractometer	Nonius-KappaCCD
radiation	$Mo_{K\alpha}$
λ [Å]	0.71073
T [K]	123
max. 2θ [°]	50
no. of data	34942
no. of unique data	13957
no. of unique data [$I > 2\sigma(I)$]	7212
no. of variables	945
no. of restraints	841
$R(F)$ for $I > 2\sigma(I)$	0.092
$wR2(F^2)$ for all data	0.280
min./max. diff. peak [e Å^{-3}]	−0.838/1.882 (in solvent DMSO)

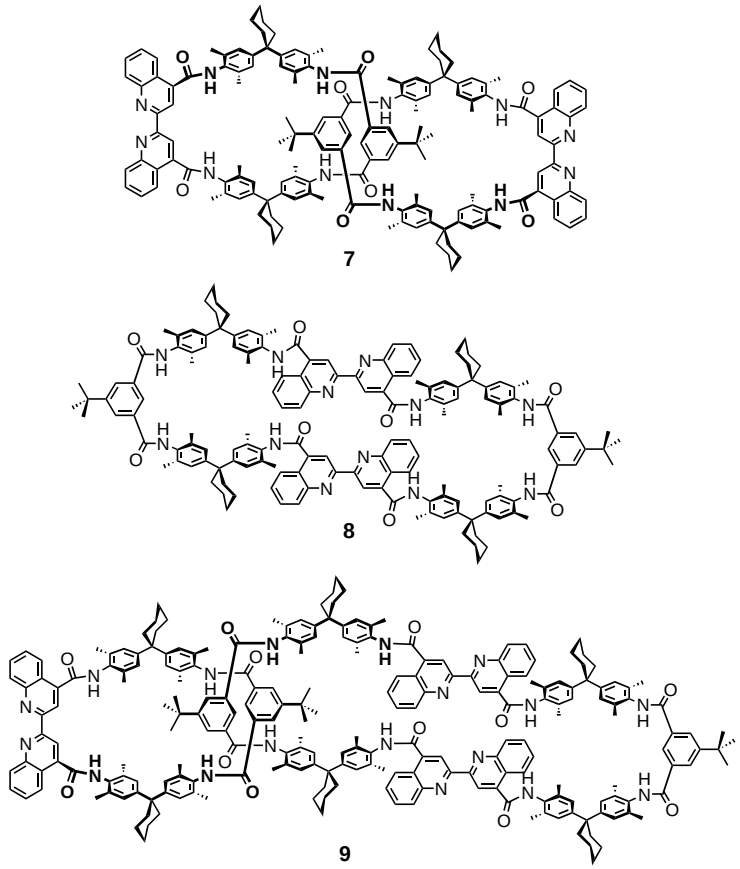

7

8

9

These results give an insight into why macrocycle **8** is formed in much greater yield in the macrocyclization as compared to the smaller analogue **6**. For the formation of **8**, a transoid conformation of **4** is advantageous, because the two isophthalic acid building blocks that come together in **8** provide sufficient curvature for closing the macrocycle, while the diamine building blocks **4** may remain in a relaxed transoid geometry. This is again supported by molecular modeling, which shows that the stretched, transoid conformation of the two biquinoline moieties is realized in the energetically most favorable conformers of **8** (Figure 2). In

0947-6539/03/0906-1334 $ 20.00+.50/0 *Chem. Eur. J.* **2003**, *9*, No. 6

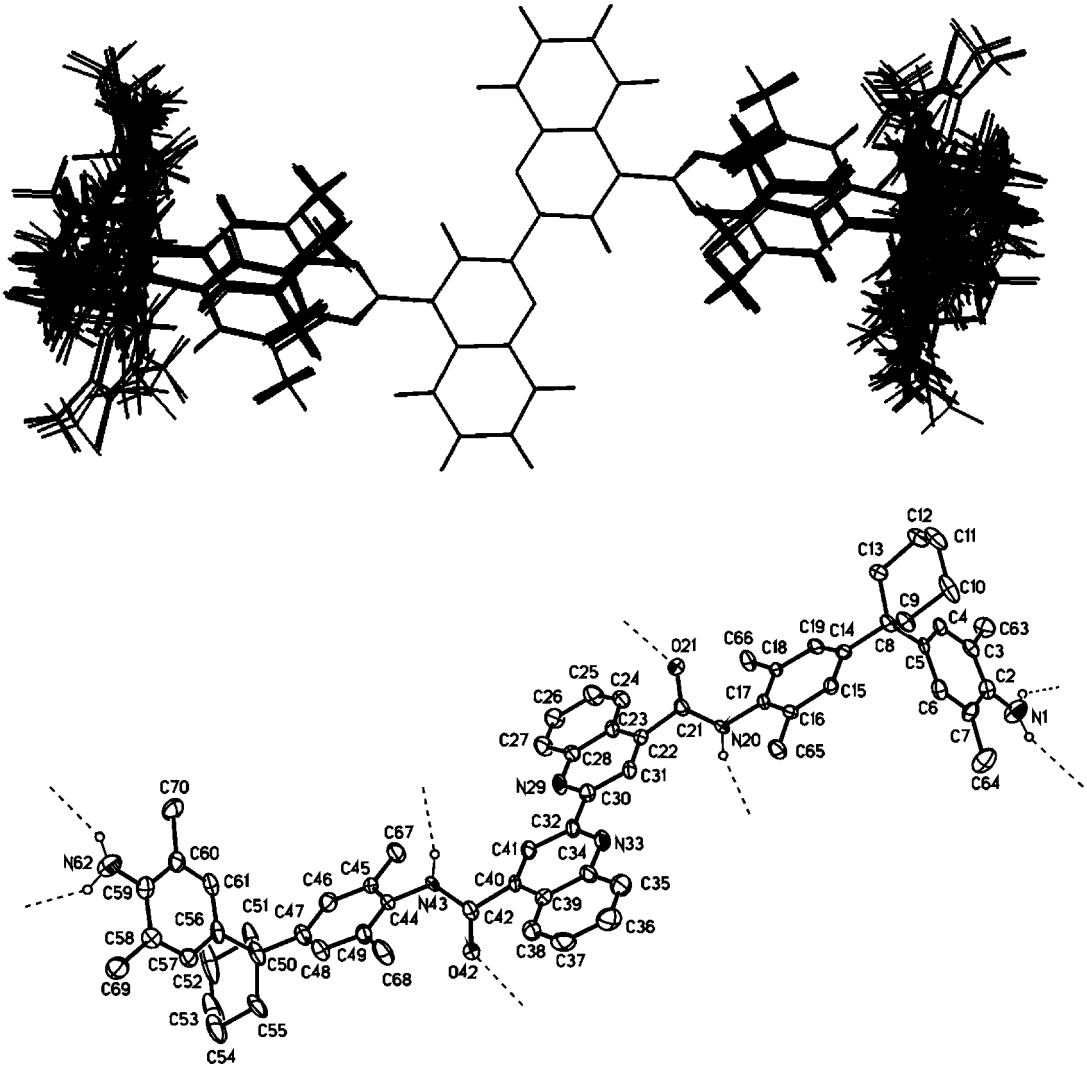

Figure 1. Top: Superposition of the 40 lowest energy conformers of **4** obtained from a Monte Carlo conformer search with 3000 steps. Bottom: Structure of intermediate **4** (ORTEP plot; 50% probability level). Carbon-centered hydrogen atoms and solvent molecules are omitted for clarity. Dotted lines indicate hydrogen bonds to adjacent molecules and DMSO incorporated in the crystal.

contrast, for ring closure to **6**, intermediate **4** needs to adopt the less favorable cisoid conformation. Thus, due to the conformational preferences of **4**, macrocycle **8** is formed more readily, even though its formation can be expected to be entropically less favorable than that of **6**.

From these considerations, coordination of the biquinoline to a metal ion such as Cu^{I} seemed like a suitable means of preorganizing building block **4** such that the macrocyclization would yield the copper complex of **6** as the main product. However, the amounts of **6** obtained after demetalation of the resulting mixture of copper complexes with potassium cyanide were disappointing and, consequently, we used the procedures outlined in Scheme 1 for the synthesis of wheel **6**.

Two catenanes, **7** and **9**, are also formed during the macrocyclization, most probably through the formation of hydrogen bonds between macrocycle **6** or **8**, respectively, already present in solution, and building block **4**. According to previous reports on X-ray structures of rotaxanes[27] and on the binding constants of different types of carbonyl compounds,[28] three hydrogen bonds mediate the template effect. Two of them connect the carbonyl group of the open-chain guest in a forked manner with two amide NH hydrogen atoms, while the third one is formed between the amide NH hydrogen of the guest and a carbonyl group on the macrocyclic host. Final capping of building block **4**, threaded into one of the two macrocycles, with isophthalic acid dichloride **5** yields the interlocked catenane structure. Since we were unable to detect a catenane built from two octalactam wheels, we suggest that the small wheel binds either building block **4** to yield catenane **7** or its analogue elongated by an isophthalic acid dichloride **5** and a second subunit **4**. The latter complex would then yield catenane **9**. Although somewhat speculative, this would imply that **6** is more favorably preorganized for mediating the template effect as compared to **8**, which is likely to be too flexible to provide favorable binding.

Rotaxane synthesis: new size requirements for the stopper groups: Among the many different template effects that are suitable for rotaxane synthesis, one of the most efficient is the

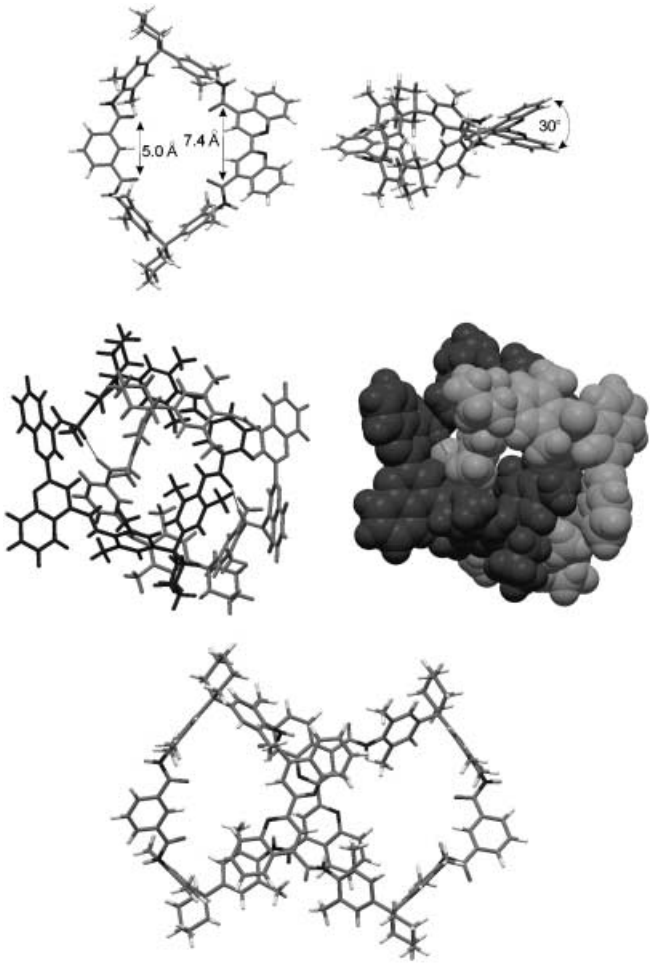

Figure 2. Lowest energy conformations (*tert*-butyl groups omitted) out of 3000 structures optimized in a Monte Carlo conformational search for tetralactam macrocycle **6** (top), catenane **7** (center), and octalactam macrocycle **8** (bottom). Some structural parameters are given for **6** to provide an idea of the increased cavity size resulting from the use of the biquinoline moiety (carbonyl – carbonyl distance 7.4 Å versus 5.0 Å) in the cisoid conformation; the two aromatic planes of the halves of the biquinoline moiety are mutually tilted by about 30°. The catenane is also shown in a space-filling representation to show how densely packed the cavities of the two macrocycles are. Note that **8** prefers a figure-eight-shaped structure that permits stacking interactions of the aromatic rings in the center of the molecule. The two biquinoline units in **8** display a transoid conformation.

anion template method established by Vögtle and co-workers.[8] However, the yield of rotaxane is strongly dependent on the particular structural features of the stopper, the axle center piece, and the wheel.[8d] Consequently, it is not clear a priori whether the new macrocycle **6** would be suitable for rotaxane synthesis and what stopper would be large enough to prevent the axle from deslipping. The biquinoline moiety is not only larger, but also more flexible than the usual isophthalic acid building blocks, due to the single bond connecting the two quinolines. Thus, somewhat larger stoppers may be required for the generation of rotaxanes. Molecular modeling supports these assumptions: while the distance between the two carbonyl carbon atoms of the isophthalic acid amide unit is about 5.0 Å, the corresponding distance in the biquinoline part amounts to about 7.4 Å (Figure 2). Accordingly, all attempts to use the standard tritylphenol stopper **12a** or its trimethyl derivative **12b** were unsuccessful. Even trityl stopper **12c** with two methylphenyl

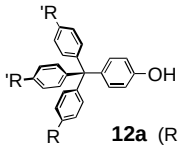

12a (R = R' = H)
12b (R = R' = Me)
12c (R = *t*Bu, R' = Me)
12d (R = R' = *t*Bu)

groups and one *tert*-butylphenyl group did not yield rotaxanes, presumably because these stoppers still can readily deslip. Finally, a rotaxane was successfully assembled with the tris(4-*tert*-butylphenyl)phenol stopper **12d**. A similar "all-or-nothing" effect has been described previously for closely related stopper groups.[14a] The rationale for such an effect is that in a first step the rotaxane wheel slips over one of the three aromatic groups of the trityl part of the stopper. In a second step, the rest of the stopper passes through the wheel and the rotaxane, if initially formed, dissociates into its free components. Such a stepwise mechanism for deslipping proceeds via two different energy barriers, both of them small enough to allow the axle to deslip even at room temperature. In the present case, this means that the presence of three *tert*-butyl groups around the tritylphenol stopper is mandatory, as realized in **12d**. Finally, the two rotaxanes **16** and **17** could be obtained by the anion template method[8] as depicted in Scheme 2. The stopper phenol is deprotonated with potassium carbonate and dibenzo[18]crown-6 (18-C-6), which is used as a solid/liquid phase-transfer catalyst. In a first step, the phenolate and one of the axle center pieces **10** or **11** form the semi-axle **13** or **14**, respectively. Also, the phenolate binds with its anionic oxygen inside macrocycle **6** by hydrogen bonding to two of the amide protons to yield the supramolecular nucleophile **15**. It is not clear as to which side of the wheel is more suitable for binding the phenolate. However, as shown in Scheme 2, we prefer the isophthalic acid amide half of the macrocycle, because it 1) presents the two amide protons at a smaller distance and 2) positions them almost in a plane, while the two amide protons on the biquinoline side are not as well preorganized due to the torsional angle about the 2-2′ single bond in the biquinoline unit. In the final step, **15** reacts with **13** or **14** in a nucleophilic displacement reaction, trapping the wheel on the axle and giving rise to the rotaxanes **16** and **17** as final products in yields of 23 and 34%, respectively.

Synthesis and molecular modeling of metal complexes: The dimeric Cu^{I} complexes **19** and **20** of the rotaxanes **16** and **17** were easily obtained in good quantities by reaction with 0.5 equivalents of $[Cu(CH_3CN)_4]PF_6$ at room temperature (Scheme 3). Similarly, the $[Cu(wheel)_2]^+$ complex **18** was also prepared. The $(bpy)_2Ru^{II}$ complex **22** also proved to be easily accessible in its racemic form by the reaction of **6** with its precursor complex **21** in refluxing ethylene glycol (Scheme 4).[29]

0947-6539/03/0906-1336 $ 20.00+.50/0 *Chem. Eur. J.* **2003**, *9*, No. 6

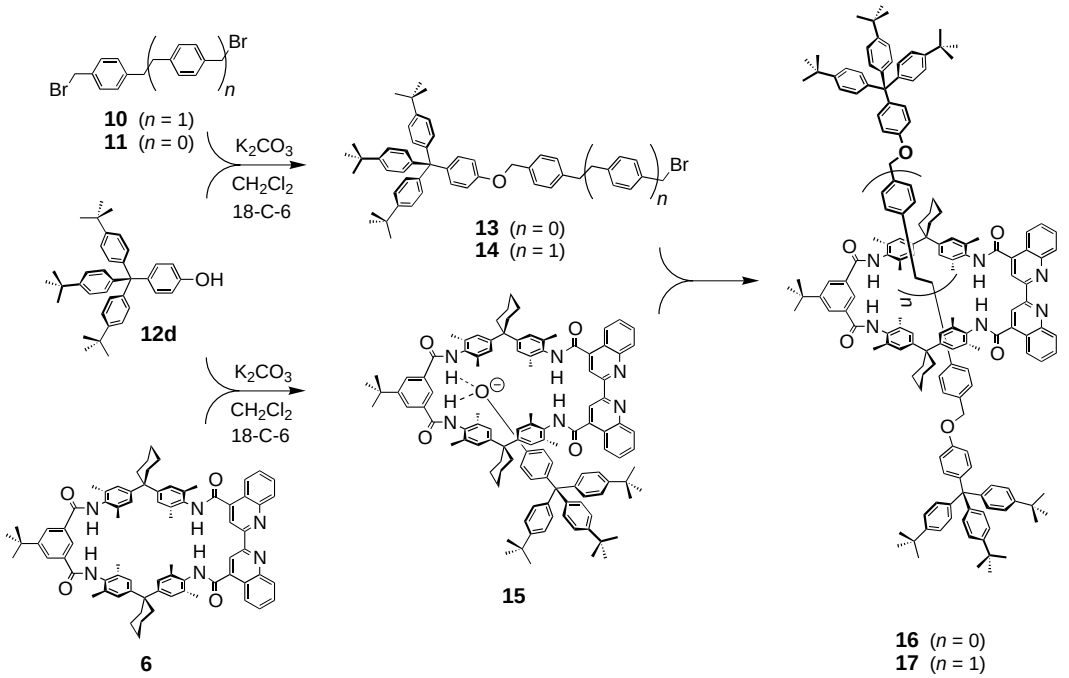

Scheme 2. Synthesis of **16** and **17**. 18-C-6 = dibenzo[18]crown-6.

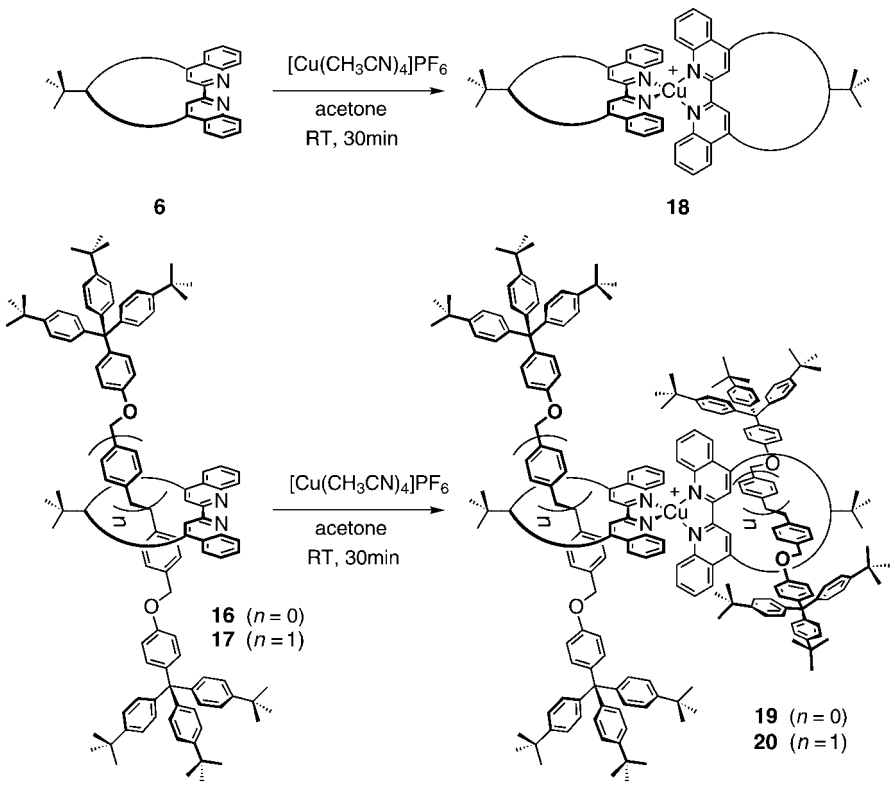

Scheme 3. Synthesis of copper complexes **18**–**20**.

To get some idea of their structures, we performed molecular dynamics calculations on the copper complexes **18**–**20** (see Scheme 3) and the $(bpy)_2Ru^{II}$ complex with the augmented MM2 force field implemented in the CACHE 5.0 program.[30] We used this program in addition to MacroModel, partly because on one hand, the latter program does not provide parameters for copper or ruthenium, but in our experience gives excellent result as far as hydrogen bonding and other noncovalent interactions are concerned. On the other hand, the augmented MM2 force field in CACHE allows us to calculate the copper complexes, but does not give as good results with respect to hydrogen bonding. To ensure comparability, we performed several test calculations on the free macrocycle **6** with CACHE as well as MacroModel. Since **6** is rather rigid and intramolecular hydrogen bonding does not play a role at all, it was no surprise that both programs gave similar results, with only small differences between the torsional angles calculated for the bond connecting the two quinoline moieties. With MacroModel, an angle of 30° was obtained, while the CACHE program generated an angle of 39°. Larger discrepancies between the two programs were obtained when modeling the catenane **7**, in which hydrogen bonding connects the two interpenetrating wheels. Also, the calculated conformations of octalactam macrocycle **8** differ somewhat with the two programs. For these molecules, it is apparent that caution needs to be exercised in comparing calculations obtained from the different programs.

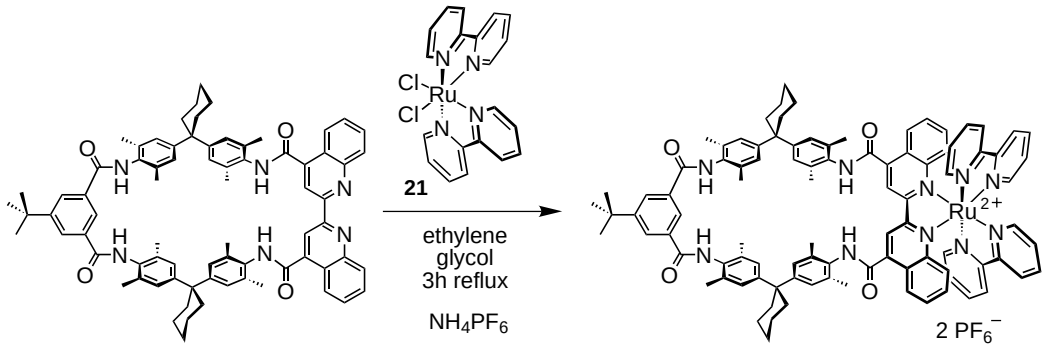

Scheme 4. Synthesis of **22**.

Figure 3 shows low-energy conformations of the dimeric Cu^I complexes **18** and **20**. The differences in conformation are easy to see. While the biquinoline unit of **6** is in a nonplanar

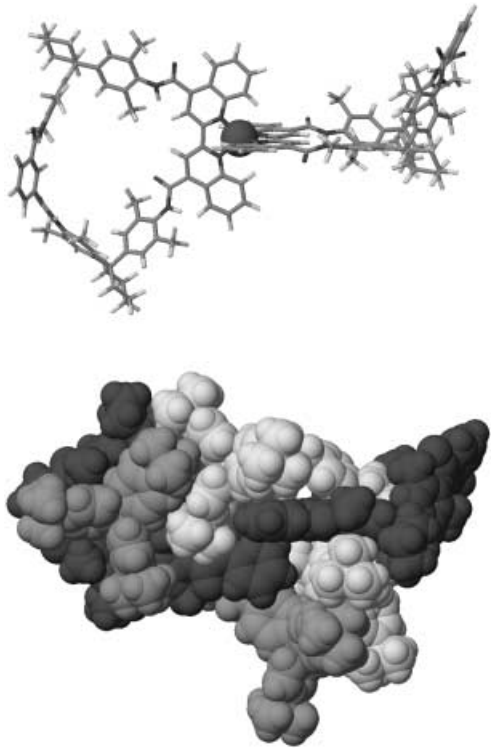

Figure 3. Dimeric Cu^I complex **18** (top: *tert*-butyl groups omitted) of wheel **6**. Note that the biquinoline unit is planarized through metal coordination in **18**. The ligand sphere around the central copper ion is typical for biquinoline complexes, with bite angles of 89°. Bottom: Space-filling representation of the dimeric rotaxane complex **20**. Note that the addition of the two rotaxane axles does not greatly affect the conformation of the two wheels, indicating that the two axles are unlikely to impose much strain on the assembly.

cisoid conformation with a torsional angle between the two aromatic planes of about 30° (see above), it is planarized upon metal coordination. In **18**, there is no significant deviation from a typical ligand sphere around the central copper ion. At 89°, the bite angle of the biquinolines is in the usual range for such metal complexes. The change in torsional angle, however, alters the overall conformation of the whole macrocycle. While **6** bears an almost helical loop arrangement, the ends of which are connected quasi-perpendicularly by the biquinoline, coordination to the metal in **18** forces the macrocycle into a bent butterfly-shaped geometry. Despite the rigid building blocks, both compounds are flexible enough to permit rotation of the four amide groups into an "in" or an "out" conformation, without causing large energy differences between the different conformers. This also holds true for the free macrocycles and catenanes.

For the rotaxane complexes **19** and **20**, the modeling approach using CACHE is again straightforward. This is because these rotaxanes are ether rotaxanes, for which hydrogen bonding between wheel and axle is of marginal importance.[28] Figure 3 shows a minimized structure for **20**, which is the reoptimized conformer of lowest energy from a series of 1000 ps dynamics trajectories at 600 K. It can clearly be seen that the wheel conformation is very similar to that of the $[Cu(wheel)_2]^+$ complex **18**. Again, the biquinoline moieties are planar. The ligand shell around the copper core is not significantly distorted. Furthermore, the two axles maximize van der Waals interactions between two stoppers by interdigitating their aromatic rings. However, such van der Waals interactions may be overestimated by the calculation, since no solvation is taken into account.

The monomeric $(bpy)_2Ru^{II}$ complex **22** has a similar overall conformation. The only notable difference to the structure of the dimeric copper complex **18** is the slightly distorted biquinoline moiety. The torsional angle about the 2,2′ bond is 9°, which is still significantly less than that in the macrocycle **6**. However, due to steric crowding around the ruthenium center, complete planarization is not achieved.

Assignment of the biquinoline conformation by ^{1}H NMR experiments: As regards the above-mentioned conformations of the biquinoline moieties, ^{1}H NMR experiments give detailed insight.[31] Although a complete assignment for the rotaxanes **16** and **17** and the corresponding copper complexes **19** and **20** is somewhat hampered by the superposition of some signals with those from the stoppers, a detailed analysis of the aromatic regions is straightforward and our assignment is in agreement with literature data.[32] Figure 4 shows the aromatic regions of the ^{1}H NMR spectra of compounds with a transoid conformation, namely building block **4** and octalactam macrocycle **8**, followed by those having a cisoid conformation,

  0947-6539/03/0906-1338 $ 20.00+.50/0

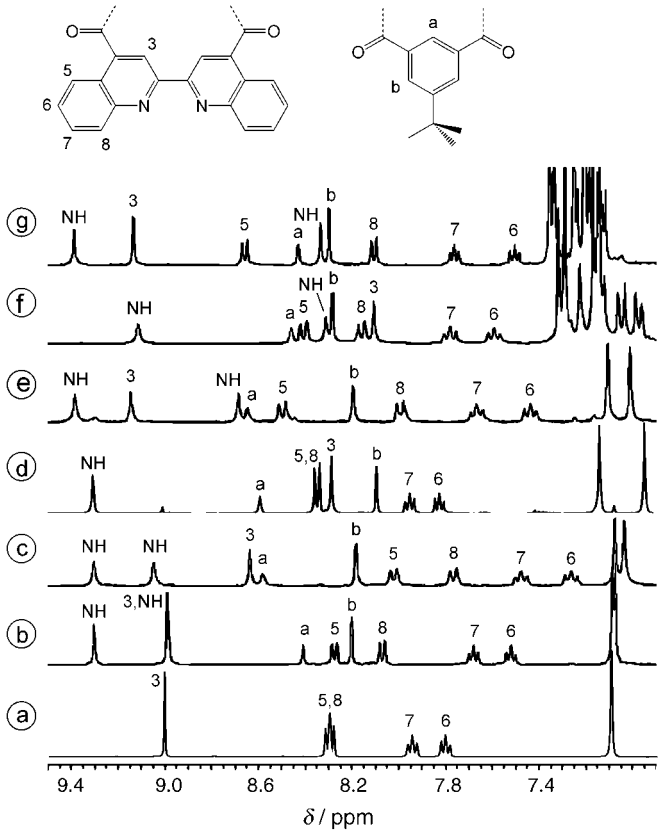

Figure 4. Aromatic regions ($\delta = 9.5-6.9$ ppm) of the ^{1}H NMR spectra of a) building block **4**, b) octalactam macrocycle **8**, c) catenane **7**, d) tetralactam wheel **6**, e) its copper complex **18**, f) rotaxane **16**, and g) the $[Cu(\mathbf{16})_2]^+$ complex **19** (bottom to top). Assignments are made as indicated in the structures shown above. Note that all spectra were recorded from samples in [D_6]acetone, except those of **4** and **6**, which were only soluble in [D_6]DMSO. Consequently, small signal shifts might occur due to differences in solvation. The assignment of the biquinoline conformation, however, is not affected by these minor shifts.

namely catenane **7**, macrocycle **6**, its copper complex **18**, rotaxane **16**, and the $[Cu(\mathbf{16})_2]^+$ dimer **19** (from bottom to top). The spectra have been deliberately arranged in such an order to facilitate comparison. The data obtained from rotaxane **17** and the corresponding copper complex **20** are very similar to those of **16** and **19** and hence are not shown. A large, conformation-dependent shift is observed for the signals for H3,3′, and hence we will now consider their chemical shifts in more detail. They appear at an almost equal chemical shift of $\delta \approx 9.0$ ppm for transoid compounds **4** and **8** (traces (a) and (b)), whereas they are observed in the range $\delta \approx 8.0-8.7$ ppm for cisoid **6**, **7**, and **16** (traces (c), (d), and (f)). The slight upfield shift of this signal for rotaxane **16** ($\delta \approx 8.1$ ppm) relative to that of macrocycle **6** ($\delta \approx 8.3$ ppm) has been observed previously[8] for other similar rotaxanes, and can be attributed to the anisotropy of the aromatic rings of the axle center pieces. In contrast, it is not quite clear as to why the signal in the spectrum of catenane **7** is shifted downfield to $\delta \approx 8.7$ ppm. Complexation with a copper ion induces a strong downfield shift back to a position around $\delta \approx 9.2$ ppm, probably due to a planarization of the biquinoline system upon metal complexation.

The amide protons, which are sometimes difficult to identify, can be unequivocally assigned by adding a small amount of deuterated methanol. These protons rapidly exchange with the methanol-OD deuterium atoms and hence their signals vanish almost completely.

Finally, we should mention that the formation of rotaxanes affects the chemical shifts of wheel protons other than H3,3′ to some extent. The signals of H6,6′, H7,7′, and H8,8′ are all subject to a small upfield shift, probably because, on average, these protons "feel" the anisotropy of the aromatic rings incorporated in the axle. Much more pronounced, however, are the effects of rotaxane formation on the signals of the axle center pieces.[14h] The anisotropy of the aromatic rings in the wheel causes upfield shifts of up to 1 ppm. In conclusion, the ^{1}H NMR spectra not only allow us to determine the conformation of the biquinoline subunit, but also permit the identification of rotaxanes and catenanes and their distinction from the macrocycles. In particular, unambiguous assignment and distinction of the catenated and macrocyclic structures is possible for **7** and **8**, respectively.

UV/Vis absorption spectra of metal complexes 18–20 and 22: Figure 5 shows the absorption spectra of the copper complexes, which are all almost identical. No significant changes

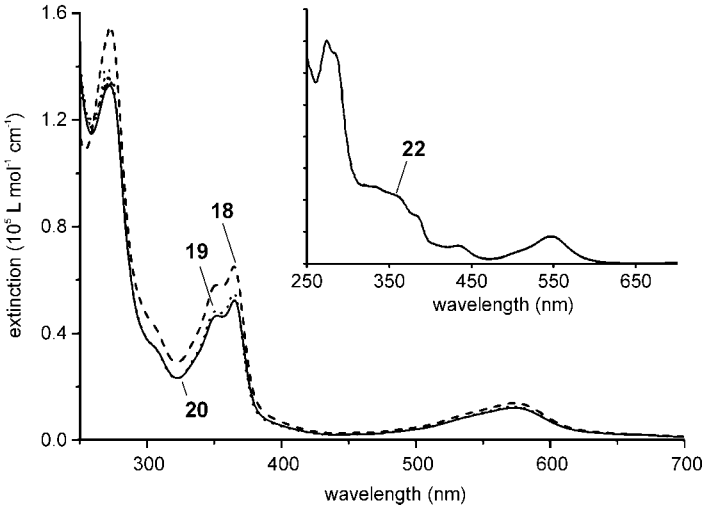

Figure 5. UV/Vis absorption spectra of **18** (dashed line), **19** (dotted line), and **20** (solid line) in dichloromethane. The inset shows the UV/Vis absorption spectrum of ruthenium complex **22** in acetonitrile.

are observed that can be attributed to the presence of the axle or its nature. Strong absorption bands are observed in the region from 250 to 400 nm, which probably correspond to ligand $\pi-\pi^*$ absorptions.[32] The band at 574 nm can be assigned to the metal-to-ligand charge transfer (MLCT) state. These spectra are very similar to that of an unsubstituted biquinoline copper(I) complex, except for some minor shifts in the peak positions.[32] For the unsubstituted biquinoline complex, the MLCT band appears at 546 nm, while for **17**–**19** it is red-shifted by about 30 nm, presumably due to the presence of the amide groups.

A previous report on a series of 3,3′-bridged biquinoline copper(I) complexes revealed the MLCT band to be strongly

dependent on the distortion of the ligand sphere from an ideal tetrahedral structure, in terms of both its wavelength and intensity.[32b] A perfectly planar conformation of the biquinoline ligands allows the π electrons to delocalize completely over both aromatic systems and thus lowers the energy level of the π* orbital. Consequently, a distortion from this ideal geometry results in a decrease in intensity and a blue shift of the MLCT band. All three Cu^{I} complexes under study here display a strong MLCT band at 574 nm, indicating a Cu(biquinoline)$_2$ core without significant distortion. Furthermore, the interlocking of the axle, with its two bulky stoppers, does not change this situation.

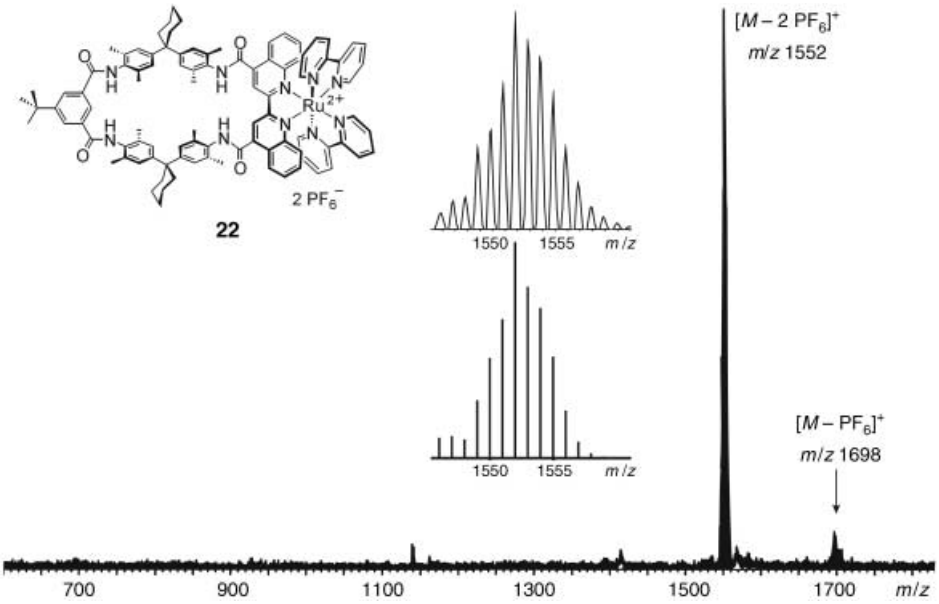

Figure 6. MALDI mass spectrum of **22** obtained with 2,5-dihydroxybenzoic acid as the matrix. The insets show the measured (top) and calculated (bottom) isotope patterns.

Mass spectrometric characterization: The macrocycles, catenanes, and rotaxanes under study here can easily be observed in their FAB and MALDI mass spectra. Usually, FAB ionization generates mainly protonated ions and to some extent induces fragmentation due to the higher internal energy imparted to the ions as compared to MALDI, which on the other hand provides protonated, sodiated, and potassiated species. The mass peaks for the catenanes and rotaxanes are accompanied by signals for the components, predominantly the wheel. For example, the large catenane **9** shows signals in its FAB spectrum corresponding to its pseudomolecular ion $[M+H]^+$ (*m*/*z* 3415) along with fragment signals at *m*/*z* 1139 for the small protonated wheel and at *m*/*z* 2277 for the larger protonated wheel. It is mainly this result that led us to the assignment of a catenated structure for **9**. The NMR spectra are complicated and not as easily interpretable. If a monocyclic species had been formed, no ready fragmentation would be expected, since two bonds would have to be broken for the generation of fragments instead of only one in the case of the catenane, followed by deslipping of the open macrocycle. At higher internal energies, a whole series of fragments would be expected for a single macrocycle, because cleavage of the first bond could be followed by cleavage of a second at many different positions. Instead, a catenane would yield only the two component macrocycles. A more detailed study[33] involving MS/MS and ion mobility experiments yielded more precise data on this matter, and therefore we refrain here from a more in-depth analysis of the mass spectra. The copper complexes yield clean MALDI spectra, which are dominated by signals corresponding to the loss of a PF_6^- counterion. Fragments due to the loss of one ligand are also observed. Similar results were obtained by ESI-MS. Finally, the $(bpy)_2Ru^{II}$ complex **22** yields a clean MALDI mass spectrum with only two prominent signals (Figure 6). One corresponds to the loss of one PF_6^- counterion (*m*/*z* 1698), the other to the loss of both counterions (*m*/*z* 1552). Interestingly, this ion, which would be expected to be doubly charged and thus should appear at *m*/*z* 776 with a spacing between the isotope peaks of 0.5 amu, is actually observed at *m*/*z* 1552 with peak distances of 1 amu and thus is singly charged. This indicates that an electron-transfer process from the PF_6^- ion to the ruthenium complex must be operative during the ionization procedure.[34] As shown for **22**, which has the most complex isotope pattern due to the ruthenium present, the experimental pattern is in good agreement with that calculated on the basis of natural abundances (Figure 6, insets). This holds true for all other species under study as well and thus confirms the elemental compositions.

To assess their potential to form larger assemblies, we tested catenane **7** and octalactam macrocycle **8** with respect to their binding behavior towards Cu^{I} by electrospray ionization mass spectrometry.[35] Equimolar mixtures of $[Cu(CH_3CN)_4]PF_6$ with either one of these species in acetone indeed resulted in the formation of copper-mediated complexes, as indicated by the purple color of the solutions, which were 50 μM when subjected to the MS experiments. To our surprise, no broad distributions of oligomeric assemblies were formed. Rather, the catenane gave a 2:2 complex of Cu^{I} and **7** accompanied by a minor signal for a 1:1 complex, while the octalactam macrocycle yielded exclusively 1:1 complexes.[33] Since it is hard to imagine how a 1:1 complex of catenane **7** and Cu^{I} might be geometrically possible in a species with all bonding sites saturated, we interpret the minor signal as a fragment resulting from the 2:2 complex. No larger complexes were observed, although these were initially expected to form to avoid steric strain within the complexes; we thus tried to find the observed complexes by molecular modeling to get an impression of their structure. The resulting structures are shown in Figure 7. According to these calculations, formation

0947-6539/03/0906-1340 $ 20.00+.50/0 *Chem. Eur. J.* **2003**, *9*, No. 6

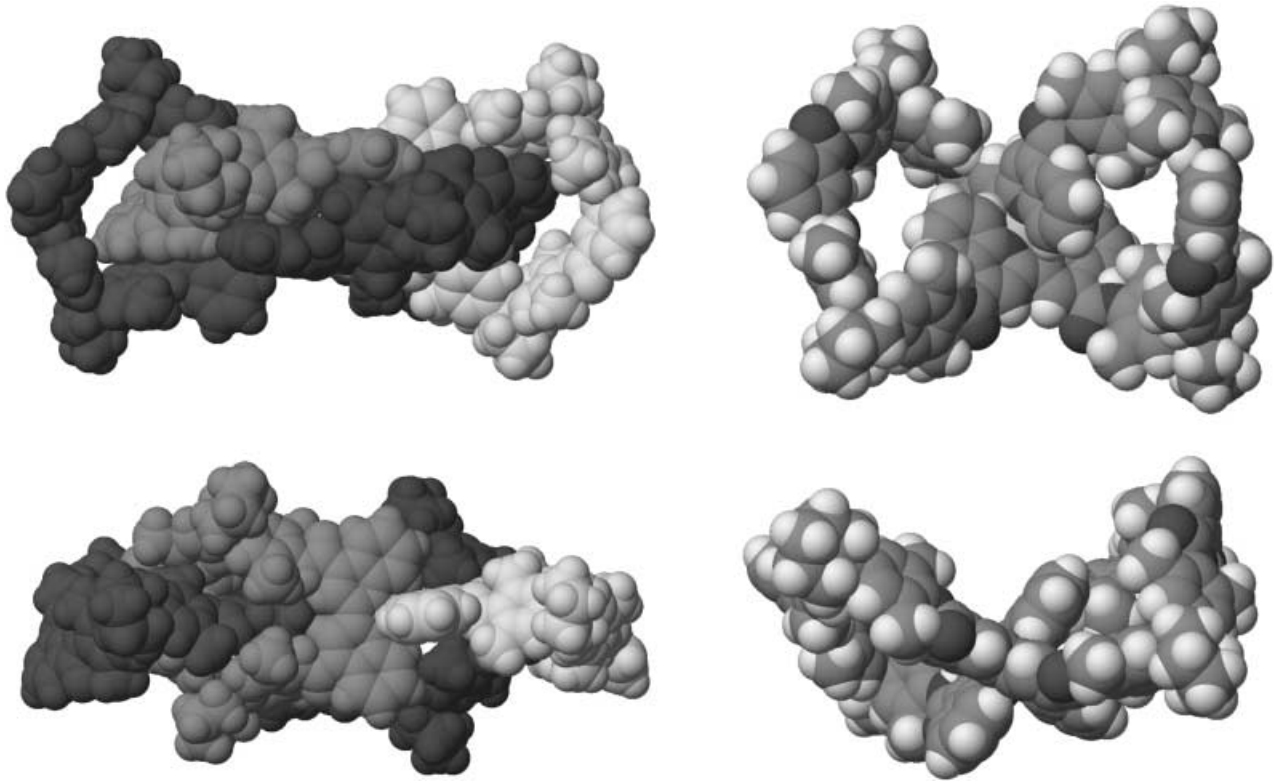

Figure 7. Assemblies of catenane **7** (left) and octalactam macrocycle **8** (right) with Cu^{I} ions, each shown in top and side views. For clarity, the rings of the catenane assembly are represented with different graytones.

of such assemblies should be possible. Catenane **7** dimerizes through two Cu^{I} ions, which are separated by a distance of about 10 Å, so that the repulsive interactions between the two positive charges are minimized. The presence of some strain is indicated by a slight distortion of the coordination sphere around the Cu^{I} ions. In contrast, macrocycle **8** binds a copper ion at its center and forms a figure-eight-shaped molecule as shown in Figure 7 (right). Seemingly, larger assemblies are not formed due to the entropic costs of assembling a larger number of molecules into one entity. These findings further support the assignment of catenated and simple macrocyclic structures to **7** and **8**.

Anion binding behavior of 22: It is well known that tetralactam macrocycles and their analogues are capable of anion binding,[36, 37] which is also reflected in the rotaxane synthesis described above. We were interested in two aspects: 1) Is anion binding with our macrocycle possible in a competitive solvent such as DMSO? 2) How does the coordination to a positively charged metal fragment change the binding abilities of macrocycle **6**?[38] To address the latter question, ^{1}H NMR titration experiments are the method of choice because they allow the direct comparison of **6** and **22** and at the same time yield qualitative information on the position of the guest.

Before performing NMR titrations, a Job analysis[39] of the stoichiometry was first performed, as shown in Figure 8 for **22**. Four proton signals were followed: the two different NH signals and the signals of CH protons pointing into the cavity of the macrocycle (H^{3} and H^{a} according to the assignment given in Figure 4). For all four protons, the maximum complex concentration was found for a molar fraction of $x = 0.5$, indicating the formation of 1:1 complexes.

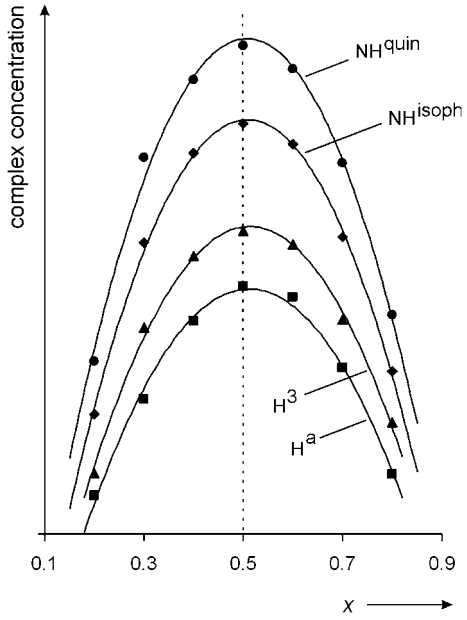

Figure 8. Job plot of solutions of **22** with tetrabutylammonium chloride as the guest salt. The maximum at a molar ratio of $x = 0.5$ indicates the formation of 1:1 complexes.

Next, NMR titrations with **6** and **22** were carried out with tetrabutylammonium chloride as the guest in DMSO. This solvent not only readily dissolves the hosts and the guest salt,

  0947-6539/03/0906-1341 $ 20.00+.50/0

but also strongly competes with the guest for hydrogen bonds and thus presents a challenge for anion binding within these hosts. The chloride anion should be small enough to fit easily into the macrocycle's cavity and should bind through two hydrogen bonds, provided that the DMSO molecules in the vicinity are not too competitive. Indeed, significant shifts are observed for several signals (Figure 9). Depending on the concentration of the guest, the signals of the amide protons move by a maximum of about 0.6 ppm for both species. This is, of course, expected, because they are directly involved in binding the anion through hydrogen-bonding interactions. However, the carbon-centered hydrogens pointing into the cavity (H^3 and H^a) also strongly "feel" the influence of the anion. This indicates the presence of the anion inside the cavity. Smaller effects on other signals are also observed. For example, the signals of the aromatic protons of the "Hunter diamine" building blocks are subject to some smaller shifts. Nevertheless, the effects on the amide protons and H^3/H^a are most pronounced and, therefore, these signals were chosen in order to gather titration data for the fitting of the binding constants.

The model used for the fitting not only included the free receptor and guest, but also a 1:1 complex of the two and a 1:2 complex in which two anions are bound to the macrocycle. This model provided the best fit of all models tested for both receptors. From the binding constants in Table 2, we can conclude that binding of the second anion ($K = 20\,\text{M}^{-1}$ in **22**, $3\,\text{M}^{-1}$ in **6**) is much weaker than that of the first ($K = 1020\,\text{M}^{-1}$ in **22**, $180\,\text{M}^{-1}$ in **6**). Otherwise, this result would not be consistent with the Job plot analysis. It is, of course, not unexpected, in view of the accumulation of negative charges inside the host cavity. The other conclusion that can be made is that chloride binds more strongly to the ruthenium complex **22** as compared to **6**. Two factors are likely to contribute to this effect: 1) the ruthenium complex is positively charged and electrostatic interactions with the anion may stabilize the host–guest complex; 2) coordination of the macrocycle to the metal center almost completely planarizes the biquinoline moiety and thus better preorganizes the two biquinoline NH groups for anion binding. In **6**, the binding of the anion must provide the necessary energy in order to force the receptor into an appropriate conformation, at the expense of its binding energy.

Table 2. Binding constants K_1 and K_2 [M^{-1}] and free association energies ΔG_1 and ΔG_2 [kJ mol^{-1}] obtained from a least-squares fit of the NMR titration data with the Specfit program for hosts **6** and **8**.[45]

Host	Guest	K_1[a] [M^{-1}]	K_2[b] [M^{-1}]	ΔG_1 [kJ mol^{-1}]	ΔG_2 [kJ mol^{-1}]
6	Cl^-	180 ± 20	3 ± 2	-12.9	-2.3
8	Cl^-	1020 ± 50	20 ± 5	-17.2	-7.0
6	$H_2PO_4^-$	420 ± 30	–	-14.9	–
8	$H_2PO_4^-$	25300 ± 300	–	-25.1	–

[a] Binding constant for the equilibrium reaction $R+S \rightleftharpoons RS$. [b] Binding constant for the equilibrium reaction $RS+S \rightleftharpoons RS_2$.

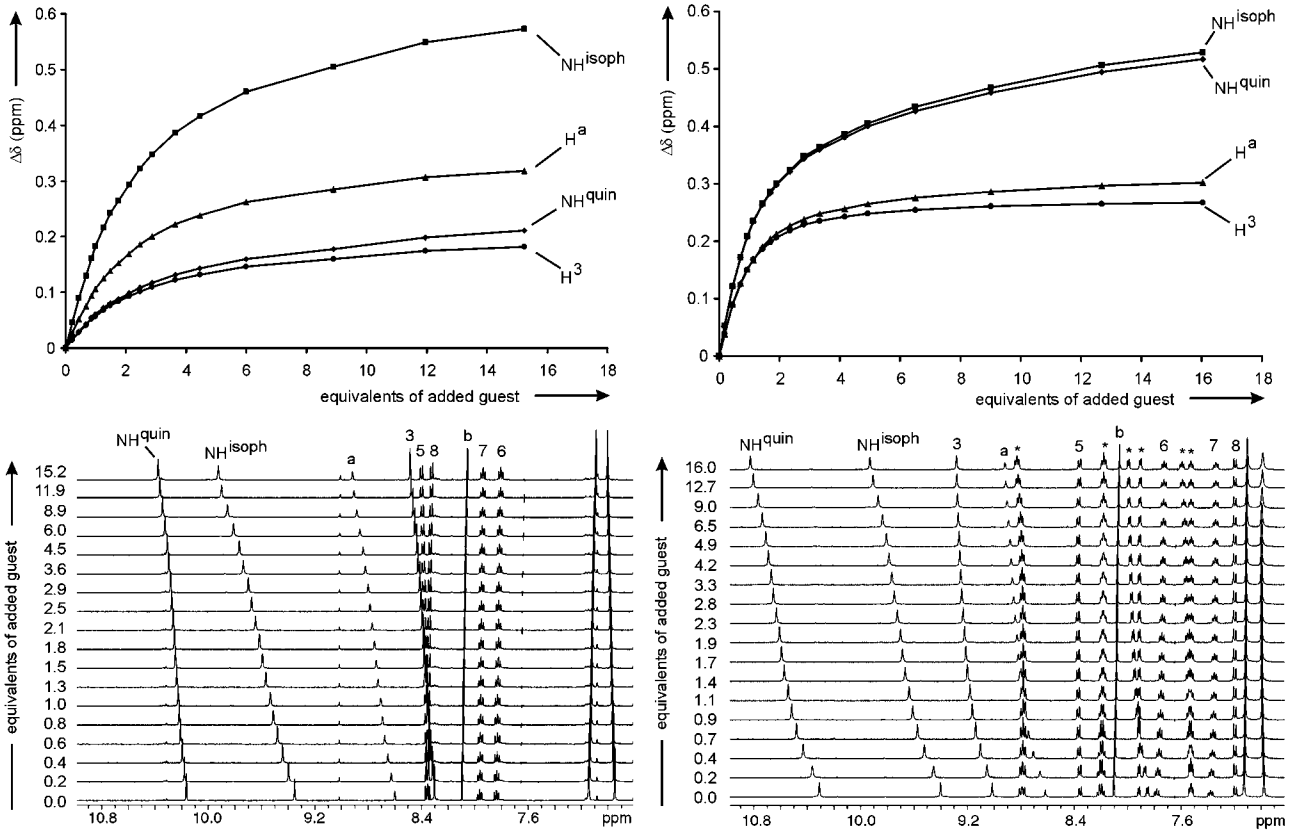

Figure 9. Bottom: Aromatic region of ^{1}H NMR titration spectra of 4 mM solutions of macrocycle **6** (left) and the corresponding Ru^{II} bipyridine complex **22** (right) in [D_6]DMSO. The guest was tetrabutylammonium chloride. The assignment of the ^{1}H NMR signals is given at the top of each series of spectra, as defined in Figure 4. Asterisks indicate signals originating from the bipyridine ligands. Top: Titration curves derived from these two series of ^{1}H NMR spectra.

0947-6539/03/0906-1342 $ 20.00+.50/0 *Chem. Eur. J.* **2003**, *9*, No. 6

Analogous experiments with dihydrogen phosphate $H_2PO_4^-$ revealed much larger shifts in the ^1H NMR signals upon titration of **8** with the anion. A particularly large shift of about $\Delta\delta = 2.5$ ppm was observed for the biquinoline NH signals of **22**. Fitting of the titration data with the model used for the chloride complexes resulted in a rather poor fit, but the situation greatly improved when a simpler model was used involving the exclusive formation of 1:1 complexes without any contribution from a 1:2 complex of host and guest. The binding constant for binding of $H_2PO_4^-$ to ruthenium complex **22** ($K = 25\,300\,M^{-1}$) is not only much greater than that for macrocycle **6** ($K = 420\,M^{-1}$), it also exceeds that of the chloride complex by a factor of about 25. Consequently, at 25 kJ mol^{-1}, the binding energy of $H_2PO_4^-$ to ruthenium complex **22** is almost twice as high as that for binding to macrocycle **6** (15 kJ mol^{-1}). Also, the differences as compared to the chloride guest are much larger for **22** (25 versus 17 kJ mol^{-1}) than for **6** (15 versus 13 kJ mol^{-1}). One might speculate that these results indicate a different binding pattern of dihydrogen phosphate as compared to chloride. The $H_2PO_4^-$ ion may bind through more than one of its oxygen atoms, which is of course impossible for chloride and may thus rationalize the large differences.

Conclusion

We have reported the synthesis of new macrocycles and catenanes. A particular feature of these species is their ability to complex metal cations at the periphery of rather rigid macrocyclic structures.[38a, 40] Conformational arguments provide an explanation as to why two different macrocycles are formed; the fact that both are accompanied by the corresponding catenanes can be rationalized in terms of Vögtle's[1h] amide template effect. We have tested these systems with respect to their ability to form rotaxanes and have determined the stopper size necessary to trap the axle in the cavity of the wheel, which is larger than in previous examples.[8] To further demonstrate the utility of these macrocycles for supramolecular applications, several metal complexes have been synthesized, the sizes of the assemblies have been determined by ESI mass spectrometry, and the anion binding behaviors of tetralactam macrocycle **6** and its $(bpy)_2Ru^{II}$ complex **22** have been compared. The latter complex shows increased binding constants due to electrostatic interactions and a favorable preorganization. In particular, dihydrogen phosphate binds with quite a high binding energy to the metal complex, even in competitive solvents such as DMSO. Consequently, we believe that these macrocycles and catenanes are interesting and valuable building blocks for supramolecular chemistry.

Experimental Section

Instruments and methods: Melting points were determined on a Reichert microscope heating unit and are uncorrected. NMR spectra were measured on Bruker AMX250 (^1H: 250 MHz, ^{13}C: 62.9 MHz), AMX400 (^1H: 400 MHz, ^{13}C: 100.6 MHz), or (for ^1H NMR titration experiments) DRX500 (^1H: 500 MHz) spectrometers. All chemical shifts are given in ppm with the solvent signals taken as internal standards; coupling constants are in hertz. FAB mass spectra were obtained with a Concept 1H mass spectrometer (Kratos) and MALDI mass spectra were recorded with a MALDI-TOF-Spec-E (Micromass). *m*-Nitrobenzylic alcohol and 2,5-dihydroxybenzoic acid, respectively, were used as matrices. To record ESI mass spectra, a Micromass Q-TOF 2 mass spectrometer equipped with a Z geometry nanospray ion source was used with acetone as the spray solvent. A Perkin-Elmer Lambda-3 B spectrometer was used to obtain UV/Vis absorption spectra.

Syntheses: All precursors for the syntheses were obtained from Aldrich or Fluka and were used as purchased. Compounds **3**,[23] **5**,[41] and **12a–d**[42] were synthesized according to well-established literature procedures. Solvents were purified by standard methods and dried if necessary. TLC was carried out on Merck silica gel 60 F_{254} plates; for column chromatography, Merck silica gel 60 with a mesh size of 63–100 μm was used. The macrocycles and rotaxanes under study gave unsatisfactory elemental analyses due to solvent molecules encapsulated in the crystals. This phenomenon is well known[8] and, even after prolonged heating in high vacuum, the solvents can still be detected in the NMR spectra. The isotope patterns obtained by MALDI-MS (and FAB-MS, if not superimposed by hydrogen losses and/or cation radicals) are, however, consistent with those calculated on the basis of natural isotope abundances and thus confirm the elemental compositions.

2,2′-Biquinoline-4,4′-dicarboxylic acid dichloride hydrochloride (2): Starting material **1** (5 g) was dissolved in the minimum volume of ethanol and converted to the hydrochloride with concentrated hydrochloric acid. The yellow precipitate was collected by filtration and carefully washed with water. The solid was dried in vacuo and then refluxed with a large excess of $SOCl_2$ and two drops of DMF for 8 h. The excess $SOCl_2$ was completely evaporated under reduced pressure. The acid chloride **2** was obtained as a pale yellow solid in 95% yield. This product was used in the next step without further purification.

***N,N′*-Bis[4-{1′-(4″-amino-3″,5″-dimethylphenyl)cyclohexyl}-2,6-dimethylphenyl]-2,2′-biquinoline-4,4′-dicarboxylic amide (4)**: A solution of 1,1-bis(4′-amino-3′,5′-dimethylphenyl)cyclohexane 3 (11.4 g, 0.035 mol) in dry dichloromethane (150 mL) and triethylamine (2 mL) was placed in a 250 mL flask. This solution was stirred at room temperature and protected from moisture by bubbling dry argon through it. 2,2′-Biquinoline-4,4′-dicarboxylic acid dichloride hydrochloride 2 (2.8 g, 0.006 mol) was then added in six portions over a period of 1 h. After the mixture had been stirred at room temperature for a further 1 h, the solvents were evaporated under reduced pressure. The residue was subjected to column chromatography on silica eluting with dichloromethane/ethyl acetate (8:1). 3.6 g of white product was obtained. Yield: 62%; m.p. 260 °C (decomp); ^1H NMR (300 MHz, $CDCl_3$): $\delta = 1.38–1.69$ (br, 12H; CH_2 of Cy), 2.10 (s, 12H; $PhCH_3$), 2.14–2.18 (br, 8H; CH_2 of Cy), 2.34 (s, 12H; $PhCH_3$), 3.30–3.70 (br, 4H; NH_2), 6.81 (s, 4H; PhH), 7.02 (s, 4H; PhH), 7.46 (s, 2H; NH), 7.60 (ddd, $J = 8.3, 8.2, 1.3$ Hz, 2H; 7,7′-biquino H), 7.76 (ddd, $J = 8.3, 8.2, 1.3$ Hz, 2H; 6,6′-biquino H), 8.20 (d, $J = 8.2$ Hz, 2H; 5,5′-biquino H), 8.42 (d, $J = 7.9$ Hz, 2H; 8,8′-biquino H), 9.04 ppm (s, 2H; 3,3′-biquino H); ^1H NMR (300 MHz, $[D_6]$DMSO): $\delta = 1.3–1.6$ (br, 12H; CH_2 of Cy), 2.06 (s, 12H; $PhCH_3$), 2.2–2.4 (br, 8H; CH_2 of Cy), 2.34 (s, 12H; $PhCH_3$), 4.29 (br, 4H; NH_2), 6.80 (s, 4H; PhH), 7.07 (s, 4H; PhH), 7.79 (dd, $J = 7.8, 7.5$ Hz, 2H; 7,7′-biquino H), 7.94 (dd, $J = 7.8, 7.5$ Hz, 2H; 6,6′-biquino H), 8.29 (d + d, 4H; 5,5′ and 8,8′-biquino H), 9.00 (s, 2H; 3,3′-biquino H), 10.27 ppm (s, 2H; NH); ^{13}C NMR ($CDCl_3$): $\delta = 14.45, 18.62, 19.09$ (CH_3); 21.12, 23.03, 26.29, 36.79 (CH_2); 116.48, 120.72, 125.09, 125.74, 126.55, 128.92, 130.39, 131.11, 134.79 (CH); 40.7, 135.26, 141.88, 144.23, 147.97, 148.88, 154.66 (Cq); 165.82 ppm (CO); MS (FAB): m/z: 952 ($[M]^+$, 100%).

11′-*tert*-Butyl-5′,17′,23′,48′,51′,54′,57′,59′-octamethyldispiro[cyclohexane-1,2′-{7′,15′,25′,34′,37′,46′-hexaazadecacyclo[45.2.2.2$^{3',6'}$.2$^{16',19'}$.2$^{21',24'}$.1$^{9',13'}$.1$^{27',35'}$.1$^{36',44'}$.0$^{28',33'}$.0$^{38',43'}$]hexaconta-3′,5′,9′,11′,13′(58′),16′,18′,21′,23′,27′,29′,31′,33′,35′(53′),36′,38′,40′,42′,44′(52′),47′,49′,50′,54′,56′,59′-pentaeicosaene-8′,14′,26′,45′-tetraone}-20′,1″-cyclohexane] (6): A solution of 5-*tert*-butyl isophthalic acid dichloride **5** (0.26 g, 1 mmol) in dry dichloromethane (250 mL) and a mixture of **4** (0.952 g, 1 mmol) and triethylamine (2 mL) in dry dichloromethane (250 mL) were simultaneously added dropwise to dry dichloromethane (1200 mL) from separate dropping funnels, while the system was kept under argon atmosphere. The addition was completed within about 8 h, and then the solution was stirred at room temperature overnight. The solvents were subsequently evaporated under reduced pressure. The residue was subjected to column chromatography on silica

eluting with a mixture of dichloromethane, ethyl acetate, and ethanol (200:65:2) ($R_f = 0.35$). 0.11 g of macrocycle **6** was obtained as a white solid from the third fraction. Yield: 11%; m.p. 310°C (decomp); ^{1}H NMR (400 MHz, [D$_6$]DMSO): $\delta = 1.32$ (s, 9H; C(CH$_3$)$_3$), 1.41–1.60 (br, 12H; CH$_2$ of Cy), 2.01 (s, 12H; PhCH$_3$), 2.03 (s, 4H; PhCH$_3$), 2.36–2.41 (br, 8H; CH$_2$ of Cy), 6.94 (s, 4H; PhH), 7.13 (s, 4H; PhH), 7.82 (t, $J = 8.3$, 8.1 Hz, 7,7′-biquino H), 7.95 (t, $J = 8.3$, 8.1 Hz, 2H; 6,6′-biquino H), 8.09 (d, $J = 1.0$ Hz, 2H; 4,6-isophth H), 8.29 (s, 2H; 3,3′-biquino H), 8.35 (d, $J = 9.2$ Hz, 4H; 5,5′,8,8′-biquino H), 8.58 (s, 1H; 2-isophth H), 9.30 (s, 2H; isophth NH), 10.11 ppm (s, 2H; biquino NH); ^{13}C NMR (100.6 MHz, [D$_6$]DMSO): $\delta =$ 13.9, 14.5, 19.1, 31.4 (CH$_3$); 23.1, 26.1, 30.5, 39.7 (CH$_2$); 118.9, 124.1, 125.5, 126.5, 127.8, 128.8, 131.1, 132.9, 134.8 (CH); 130.6, 135.5, 143.5, 148.7, 149.1, 152.7, 156.7 (Cq); 165.1, 165.4 ppm (CO); MS (FAB): m/z: 1139 ([M+H]$^+$, 100%).

The same reaction yielded three other fractions, one of which contained catenane **7** built from two macrocycles **6** ($R_f = 0.82$, CH$_2$Cl$_2$/EtOAc, 8:1). The second fraction corresponded to the octalactam macrocycle **8** ($R_f =$ 0.56, CH$_2$Cl$_2$/EtOAc, 8:1), bearing four "Hunter diamines" **3** in addition to two isophthalic acid and two biquinoline building blocks. Finally, catenane **9** was collected from the third fraction.

[2]-{11′-*tert*-Butyl-5′,17′,23′,48′,51′,54′,57′,59′-octamethyldispiro[cyclohexane-1,2′-{7′,15′,25′,34′,37′,46′-hexaazadecacyclo[45.2.2.2$^{3'.6'}$.2$^{16'.19'}$.2$^{21'.24'}$.1$^{9'.13'}$.1$^{27'.35'}$.1$^{36'.44'}$.0$^{28'.33'}$.0$^{38'.43'}$]hexaconta-3′,5′,9′,11′,13′(58′),16′,18′,21′,23′,27′,29′,31′,33′,35′(53′),36′,38′,40′,42′,44′(52′),47′,49′,50′,54′,56′,59′-pentaeicosaene-8′,14′,26′,45′-tetraone}-20′,1″-cyclohexane]}-{11′-*t*-butyl-5′,17′,23′,48′,51′,54′,57′,59′-octamethyldispiro[cyclohexane-1,2′-{7′,15′,25′,34′,37′,46′-hexaazadecacyclo[45.2.2.2$^{3'.6'}$.2$^{16'.19'}$.2$^{21'.24'}$.1$^{9'.13'}$.1$^{27'.35'}$.1$^{36'.44'}$.0$^{28'.33'}$.0$^{38'.43'}$]hexaconta-3′,5′,9′,11′,13′(58′),16′,18′,21′,23′,27′,29′,31′,33′,35′(53′),36′,38′,40′,42′,44′(52′),47′,49′,50′,54′,56′, 59′-pentaeicosaene-8′,14′,26′,45′-tetraone}-20′,1″-cyclohexane]}catenane (7): Yield: 1%; m.p. >300°C; ^{1}H NMR (400 MHz, [D$_6$]acetone): $\delta = 1.23$ (s, 18H; C(CH$_3$)$_3$), 1.35–1.60 (br, 24H; CH$_2$ of Cy), 1.92 (s, 24H; PhCH$_3$), 7.06 (s, 24H; PhCH$_3$), 2.24 (br, 16H; CH$_2$ of Cy), 7.02 (s, 8H; PhH), 7.06 (s, 8H; PhH), 7.24 (t, $J = 7.63$ Hz, 4H; 7,7′-biquino H), 7.46 (t, $J = 7.82$ Hz, 4H; 6,6′-biquino H), 7.74 (d, $J = 8.48$ Hz, 4H; 8,8′-biquino H), 8.00 (d, $J = 8.29$ Hz, 4H; 5,5′-biquino H), 8.16 (d, $J = 1.13$ Hz, 4H; 4,6-isophth H), 8.56 (s, 2H; 2-isophth H), 8.62 (s, 4H; 3,3′-biquino H), 9.03 (4H; isophth NH), 9.29 ppm (s, 4H; biquino NH); ^{13}C NMR (100.6 MHz, [D$_6$]acetone): $\delta = 14.46$, 18.92, 19.07 (CH$_3$); 23.82, 28.75, 31.31, 31.52, 37.7 (CH$_2$); 117.1, 125.8, 127.5, 128.8, 130.7, 132.6 (CH); 35.7, 54.47, 57.1, 135.7, 136.0, 136.4, 148.7, 155.1 (Cq); 165.8, 166.8 ppm (CO); MS (MALDI): 2313 ([M+K]$^+$, 30%), 2299 ([M+Na]$^+$, 70%), 2277 ([M+H]$^+$, 100%).

42′,91′-Di-*tert*-butyl-5′,30′,36′,48′,54′,79′,85′,97′,100′,102′,105′,108′,111′,113′,116′,119′-hexadecamethyltetraspiro[cyclohexane-1,2′-cyclohexane-1″,33′-cyclohexane-1‴,51′-cyclohexane-1⁗,82′-7′,16′,19′,28′,38′,46′,56′,65′,68′,77′,87′,95′-dodecaaza-nonadecacyclo[94.2.2.2$^{3'.6'}$.2$^{29'.32'}$.2$^{34'.37'}$.2$^{47'.56'}$.2$^{52'.55'}$.2$^{78'.81'}$.2$^{83'.86'}$.1$^{9'.17'}$.1$^{18'.26'}$.1$^{40'.44'}$.1$^{58'.66'}$.1$^{67'.75'}$.1$^{89'.93'}$.0$^{10'.15'}$.0$^{20'.25'}$.0$^{59.64'}$.0$^{69'.74'}$]hectacosa-3′,5′,9′(118′),10′, 12′,14′,16′,18′(117′),19′,21′,23′,25′,29′,31′,34′,36′,40′(112′),41′,43′,47′,49′,52′,54′,58′(107′),59′,61′,63′,65′,67′(106′),68′,70′,72′,74′,78′,80′,83′,85′,89′(101′),90′,92′,96′,98′,99′,102′,104′,108′,110′,113′,115′,119′-pentacontaene-8′,27′,39′,45′,57′, 76′,88′,94′-octaone] (8): Yield: 32%; m.p. > 300°C; ^{1}H NMR (400 MHz, [D$_6$]DMSO): $\delta = 1.40$ (s, 18H; C(CH$_3$)$_3$), 1.45–1.62 (br, 24H; CH$_2$ of Cy), 2.20 (s, 24H; PhCH$_3$), 2.30 (br, 16H; CH$_2$ of Cy), 2.36 (s, 24H; PhCH$_3$), 7.15 (s, 8H; PhH), 7.16 (s, 8H; PhH), 7.74 (t, $J = 7.75$ Hz, 4H; 6,6′-biquino H), 7.85 (t, $J = 7.58$ Hz, 4H; 7,7′-biquino H), 8.20 (d, $J = 1.01$ Hz, 4H; 4,6-isophth H), 8.25–8.30 (d + d, 8H; 5,5′- and 8,8′-biquino H), 8.34 (s, 2H; 2-isophth H), 9.04 (s, 4H; 3,3′-biquino H), 9.78 (s, 4H; isophth NH), 10.29 ppm (s, 4H; biquino NH); ^{13}C NMR (100.6 MHz, [D$_6$]DMSO): $\delta = 18.88$, 19.08 (CH$_3$); 23.01, 26.18, 29.64, 29.83, 30.02, 30.22, 30.41, 30.60, 30.79, 36.62 (CH$_2$); 116.4, 124.60, 125.10, 125.75, 126.58, 126.64, 127.48, 128.85, 130.34, 131.03, 132.12, 132.96 (CH); 35.2, 45.12, 135.10, 135.51, 144.13, 146.54, 147.94, 151.89, 154.56, 155.51 (Cq); 165.78, 165.19 ppm (CO); MS (MALDI): m/z: 2313 ([M+K]$^+$, 33%), 2299 ([M+Na]$^+$, 100%), 2277 ([M+H]$^+$, 75%).

[2]-{11′-*tert*-Butyl-5′,17′,23′,48′,51′,54′,57′,59′-octamethyldispiro[cyclohexane-1,2′-{7′,15′,25′,34′,37′,46′-hexaazadecacyclo[45.2.2.2$^{3'.6'}$.2$^{16'.19'}$.2$^{21'.24'}$.1$^{9'.13'}$.1$^{27'.35'}$.1$^{36'.44'}$.0$^{28'.33'}$.0$^{38'.43'}$]hexaconta-3′,5′,9′,11′,13′(58′),16′,18′,21′,23′,27′,29′,31′,33′,35′(53′),36′,38′,40′,42′,44′(52′),47′,49′,50′,54′,56′,59′-pentaeicosaene-8′,14′,26′,45′-tetraone}-20′,1″-cyclohexane]}-{42′,91′-di-*tert*-butyl-5′,30′,36′,48′,54′,79′,85′,97′,100′,102′,105′,108′,111′,113′,116′,119′-hexadecamethyltetraspiro[cyclohexane-1,2′-cyclohexane-1″,33′-cyclohexane-1‴,51′-cyclohexane-1⁗,82′-7′,16′,19′,28′,38′,46′,56′,65′,68′,77′,87′,95′-dodecaazanonadecacyclo[94.2.2.2$^{3'.6'}$.2$^{29'.32'}$.2$^{34'.37'}$.2$^{47'.56'}$.2$^{52'.55'}$.2$^{78'.81'}$.2$^{83'.86'}$.1$^{9'.17'}$.1$^{18'.26'}$.1$^{40'.44'}$.1$^{58'.66'}$.1$^{67'.75'}$.1$^{89'.93'}$.0$^{10'.15'}$.0$^{20'.25'}$.0$^{59.64'}$.0$^{69'.74'}$]hectacosa-3′,5′,9′(118′),10′,12′,14′,16′,18′(117′),19′,21′,23′,25′,29′,31′,34′,36′,40′(112′),41′,43′,47′,49′,52′,54′,58′(107′),59′,61′,63′,65′,67′(106′),68′,70′,72′,74′,78′,80′,83′,85′,89′(101′),90′,92′,96′,98′,99′,102′,104′, 108′,110′,113′,115′,119′-pentacontaene-8′,27′,39′,45′,57′,76′,88′,94′-octaone] catenane (9): This catenane yields rather complicated ^{1}H and ^{13}C NMR spectra which we were unable to fully interpret. Our structural assignment is based on 1) the MALDI mass spectrum (see discussion above) and 2) several clearly discernible signals in the ^{1}H NMR spectrum indicating a 1:2 ratio of two similar components. For example, the methyl groups of the "Hunter diamine" building blocks appear as four singlets in a 1:2:1:2 ratio at $\delta = 2.38$, 2.36, 2.21, and 2.09.

General procedure for the synthesis of rotaxanes: A 50 mL flask was charged with macrocycle **6** (0.1 mmol), the axle center piece (1,2-di-4-bromomethylphenylethane **10** for **16**; 1,4-dibromomethylbenzene **11** for **17**) (0.2 mmol), 4-[tris(4-*tert*-butyl)phenylmethyl]phenol **12d** (0.4 mmol), dibenzo[18]crown-6 (20 mg), anhydrous potassium carbonate (100 mg), and dry dichloromethane (30 mL). The mixture was stirred at room temperature under the protection of argon for seven days. The solids were then removed by filtration and the filtrate was concentrated under reduced pressure. The residue was subjected to column chromatography on silica gel. The column was eluted with a mixture of dichloromethane and ethyl acetate (8:1). The third fraction ($R_f = 0.22$ for **16** and 0.28 for **17**) was collected.

[2]-{4,4′-Bis[tris(4-*tert*-butylphenyl)methylphenyloxymethyl]-1,1′-bibenzyl}-{11′-*tert*-butyl-5′,17′,23′,48′,51′,54′,57′,59′-octamethyldispiro[cyclohexane-1,2′-{7′,15′,25′,34′,37′,46′-hexaazadecacyclo[45.2.2.2$^{3'.6'}$.2$^{16'.19'}$.2$^{21'.24'}$.1$^{9'.13'}$.1$^{27'.35'}$.1$^{36'.44'}$.0$^{28'.33'}$.0$^{38'.43'}$]hexaconta-3′,5′,9′,11′,13′(58′),16′,18′,21′,23′,27′,29′,31′,33′,35′(53′),36′,38′,40′,42′,44′(52′),47′,49′,50′,54′,56′,59′-pentaeicosaene-8′,14′,26′,45′-tetraone}-20′,1″-cyclohexane]}rotaxane (16): Yield 23%; m.p. > 300°C; ^{1}H NMR (400 MHz, [D$_6$]acetone): $\delta = 1.25$ (s, 54H; C(CH$_3$)$_3$), 1.41 (s, 9H; C(CH$_3$)$_3$), 1.47–1.74 (br, 12H; CH$_2$ of Cy), 2.03 (s, 12H; PhCH$_3$), 2.13 (s, 12H; PhCH$_3$), 2.24–2.48 (br, 8H; CH$_2$ of Cy), 2.59 (br, 4H; PhCH$_2$), 4.41 (s, 4H; PhCH$_2$O), 6.55 (d, $J = 9.0$ Hz, 4H; PhH), 6.78–7.33 (m, 44H; PhH), 7.54 (t, $J = 7.2$ Hz, 2H; 7,7′-biquino H), 7.73 (t, $J = 7.2$ Hz, 2H; 6,6′-biquino H), 8.06 (s, 2H; 3,3′-biquino H), 8.11 (d, $J =$ 8.4 Hz, 2H; 8,8′-biquino H), 8.23 (d, $J = 1.0$ Hz, 2H; 4,6-isophth H), 8.26 (s, 2H; isophth NH), 8.36 (d, $J = 8.4$ Hz, 2H; 5,5′-biquino H), 8.41 (s, 1H; 2-isophth H), 9.08 ppm (s, 2H; biquino NH); ^{13}C NMR (100.6 MHz, [D$_6$]acetone): $\delta = 18.9$, 19.3, 19.7, 31.6, 31.7 (CH$_3$); 23.7, 27.1, 29.1, 29.3, 29.6, 29.8, 30.1, 30.3, 30.6, 37.6, 70.1 (CH$_2$); 125.0, 126.4, 127.4, 127.6, 128.6, 128.8, 129.0, 129.3, 132.7, 132.8 (CH); 34.8, 46.0, 119.3, 131.2, 131.3, 131.4, 133.5, 135.6, 135.8, 135.9, 136.0, 140.4, 142.2, 144.7, 145.3, 149.0, 149.2, 149.8, 156.6, 157.6 (Cq); 165.5, 165.7 ppm (CO); MS (MALDI): m/z: 2388 ([M+K]$^+$, 30%), 2372 ([M+Na]$^+$, 100%), 2350 ([M+H]$^+$, 70%), 1140 (**6**+H$^+$, 100%).

[2]-{1,4-Bis[tris(4-*tert*-butylphenyl)methylphenyloxymethyl]benzene}-{11′-*tert*-butyl-5′,17′,23′,48′,51′,54′,57′,59′-octamethyldispiro[cyclohexane-1,2′-{7′,15′,25′,34′,37′,46′-hexaazadecacyclo[45.2.2.2$^{3'.6'}$.2$^{16'.19'}$.2$^{21'.24'}$.1$^{9'.13'}$.1$^{27'.35'}$.1$^{36'.44'}$.0$^{28'.33'}$.0$^{38'.43'}$]hexaconta-3′,5′,9′,11′,13′(58′),16′,18′,21′,23′,27′,29′,31′,33′,35′(53′),36′,38′,40′,42′,44′(52′),47′,49′,50′,54′,56′,59′-pentaeicosaene-8′,14′,26′,45′-tetraone}-20′,1″-cyclohexane]}rotaxane (17): Yield: 34%; m.p. > 300°C; ^{1}H NMR (400 MHz, [D$_6$]acetone): $\delta = 1.24$ (s, 54H; C(CH$_3$)$_3$), 1.41 (s, 9H; C(CH$_3$)$_3$), 1.50–1.78 (br, 12H; CH$_2$ of Cy), 2.06 (s, 12H; PhCH$_3$), 2.16 (s, 12H; PhCH$_3$), 2.29–2.50 (br, 8H; CH$_2$ of Cy), 4.30 (s, 4H; PhCH$_2$O), 6.49 (d, $J = 9.9$ Hz, 4H; PhH), 6.8–7.30 (m, 40H; PhH), 7.43 (t, $J = 7.4$ Hz, 2H; 7,7′-biquino H), 7.63 (t, $J = 7.5$ Hz, 2H; 6,6′-biquino H), 7.97–8.01 (s + d, $J = 8.2$ Hz, 4H; 3,3′- and 8,8′-biquino H), 8.22 (d, $J =$ 1.0 Hz, 2H; 4,6-isophth H), 8.27 (d, $J = 8.3$ Hz, 2H; 5,5′-biquino H), 8.38 (s, 2H; isophth NH), 8.46 (s, 1H; 2-isophth H), 9.24 ppm (s, 2H; biquino NH); ^{13}C NMR (100.6 MHz, [D$_6$]acetone): $\delta = 14.5$, 19.2, 19.8, 20.8, 31.6 (CH$_3$); 23.9, 27.2, 29.0, 29.3, 29.6, 29.9, 30.1, 30.4, 30.6, 37.2, 70.0 (CH$_2$); 114.3, 119.0, 124.9, 125.0, 126.3, 127.6, 127.7, 128.9, 132.9, 133.6 (CH); 34.9, 46.0, 52.3, 131.0, 131.2, 135.6, 135.9, 136.2, 137.7, 140.4, 144.9, 149.2, 149.7, 145.3, 155.9, 157.6 (Cq); 165.7, 165.8 ppm (CO); MS (MALDI): m/z: 2289 ([M+K]$^+$, 30%), 2272 ([M+Na]$^+$, 100%), 2250 ([M+H]$^+$, 55%), 1140 (**6**+H$^+$, 100%).

General procedure for the preparation of Cu^I complexes: The ligand (0.02 mmol) and [Cu(CH$_3$CN)$_4$]PF$_6$ (0.01 mmol) were dissolved in acetone (10 mL), and the mixture was stirred at room temperature for 30 min. The

0947-6539/03/0906-1344 $ 20.00+.50/0 *Chem. Eur. J.* **2003**, *9*, No. 6

solvent was then evaporated under reduced pressure. The purple solid was washed several times with diethyl ether and then dissolved in the minimum volume of dichloromethane. Upon slow addition of hexane, the product precipitated. This procedure was repeated at least three times in order to obtain a pure product.

Bis-{11′-*tert*-butyl-5′,17′,23′,48′,51′,54′,57′,59′-octamethyldispiro[cyclohexane-1,2′-{7′,15′,25′,34′,37′,46′-hexaazadecacyclo[45.2.2.2$^{3'.6'}$.2$^{16'.19'}$.2$^{21'.24'}$.1$^{9'.13'}$.1$^{27'.35'}$.1$^{36'.44'}$.0$^{28'.33'}$.0$^{38'.43'}$]hexaconta-3′,5′,9′,11′,13′(58′),16′,18′,21′,23′,27′,29′,31′,33′,35′(53′),36′,38′,40′,42′,44′(52′),47′,49′,50′,54′,56′,59′-pentaeicosaene-8′,14′,26′, 45′-tetraone}-20′,1″-cyclohexane]} copper(I) hexafluorophosphate (18): Yield 75%; ^{1}H NMR (400 MHz, [D$_6$]acetone): $\delta = 1.47$ (s, 18H; C(CH$_3$)$_3$), 1.58–1.76 (br, 24H; CH$_2$ of Cy), 2.28 (s, 24H; PhCH$_3$), 2.42 (s, 24H; PhCH$_3$), 2.43–2.58 (br, 16H; CH$_2$ of Cy), 7.10 (s, 8H; PhH), 7.21 (s, 8H; PhH), 7.48 (t, $J = 8.1$ Hz, 4H; 7,7′-biquino H), 7.75 (t, $J = 8.1$ Hz, 4H; 6,6′-biquino H), 8.10 (d, $J = 8.4$ Hz, 2H; 8,8′-biquino H), 8.29 (d, $J = 1.2$ Hz, 4H; 4,6-isophth H), 8.6 (d, $J = 8.4$ Hz, 4H; 5,5′-biquino H), 8.75 (s, 2H; 2-isophth H), 8.78 (s, 4H; isophth NH), 9.3 (s, 2H; 3,3′-biquino H), 9.49 ppm (s, 4H; biquino NH); ^{13}C NMR (100.6 MHz, [D$_6$]acetone): $\delta =$ 19.0, 19.4, 23.8, 27.1, 31.5, 35.8, 37.4, 46.4, 119.5, 127.0, 127.5, 127.9, 128.9, 129.2, 129.3, 130.8, 132.4, 133.0, 133.7, 135.6, 136.2, 136.8, 146.6, 147.0, 150.3, 153.0, 153.7, 155.5, 157.2, 165.2, 165.5 ppm; MS (MALDI): m/z: 2341 ([M – PF$_6$]$^+$).

Bis{[2]{4,4′-Bis[tris(4-*tert*-butylphenyl)methylphenyloxymethyl]-1,1′-bibenzyl}-{11′-*tert*-butyl-5′,17′,23′,48′,51′,54′,57′,59′-octamethyldispiro[cyclohexane-1,2′-{7′,15′,25′,34′,37′,46′-hexaazadecacyclo[45.2.2.2$^{3'.6'}$.2$^{16'.19'}$.2$^{21'.24'}$.1$^{9'.13'}$.1$^{27'.35'}$.1$^{36'.44'}$.0$^{28'.33'}$.0$^{38'.43'}$]hexaconta-3′,5′,9′,11′,13′(58′),16′,18′,21′,23′,33′,35′(53′),36,29′,31′,prime;,38′,40′,42′,44′(52′),47′,49′,50′,54′,56′,59′-pentaeicosaene-8′,14′,26′,45′-tetraone}-20′,1″-cyclohexane]}rotaxanato}copper(I) hexafluorophosphate (19): Yield 36%; ^{1}H NMR (400 MHz, [D$_6$]acetone): $\delta = 1.27$ (s, 108H; C(CH$_3$)$_3$), 1.44 (s, 18H; C(CH$_3$)$_3$), 1.54–1.71 (br, 24H; CH$_2$ of Cy), 2.05 (s, 24H; PhCH$_3$), 2.16 (s, 24H; PhCH$_3$), 2.24–2.52 (br, 16H; CH$_2$ of Cy), 2.69 (br, 8H; PhCH$_2$), 4.35 (s, 8H; PhCH$_2$O), 6.58 (d, $J = 8.8$ Hz, 4H; PhH), 7.02–7.32 (m, 62H; PhH), 7.43 (t, $J = 7.3$ Hz, 4H; 7,7′-biquino H), 7.71 (t, $J = 7.3$ Hz, 4H; 6,6′-biquino H), 8.04 (d, $J = 8.1$ Hz, 4H; 8,8′-biquino H), 8.23 (d, $J = 1.3$ Hz, 4H; 4,6-isophth H), 8.27 (s, 4H; isophth NH), 8.36 (s, 2H; 2-isophth H), 8.59 (d, $J = 8.1$ Hz, 4H; 5,5′-biquino H), 9.07 (s, 4H; 3,3′-biquino H), 9.32 ppm (s, 4H; biquino NH); ^{13}C NMR (100.6 MHz, [D$_6$]acetone): $\delta = 19.0$, 19.5, 23.8, 29.2, 29.4, 29.6, 29.7, 31.5, 34.8, 37.8, 119.6, 127.6, 127.8, 128.7, 129.0, 129.4, 132.4, 132.8, 133.0, 133.6, 135.7, 135.9, 136.0, 140.4, 142.6, 145.3, 146.4, 147.0, 149.2, 152.8, 164.9, 165.7 ppm; MS (MALDI): m/z: 4771 ([M – PF$_6$]$^+$), 2417 ([M – **16** – PF$_6$]$^+$).

Bis{[2]{1,4-Bis[tris-(4-*tert*-butylphenyl)methylphenyloxymethyl]benzene}-{11′-*tert*-butyl-5′,17′,23′,48′,51′,54′,57′,59′-octamethyldispiro[cyclohexane-1,2′-{7′,15′,25′,34′,37′,46′-hexaazadecacyclo[45.2.2.2$^{3'.6'}$.2$^{16'.19'}$.2$^{21'.24'}$.1$^{9'.13'}$.1$^{27'.35'}$.1$^{36'.44'}$.0$^{28'.33'}$.0$^{38'.43'}$]hexaconta-3′,5′,9′,11′,13′(58′),16′,18′,21′,23′,27′,29′,31′,33′,35′(53′),36′,38′,40′,42′,44′(52′),47′,49′,50′,54′,56′,59′-pentaeicosaene-8′,14′,26′,45′-tetraone}-20′,1″-cyclohexane]}rotaxanato copper(I) hexafluorophosphate (20): Yield 54%; ^{1}H NMR (400 Hz, [D$_6$]acetone): $\delta = 1.27$ (s, 108H; C(CH$_3$)$_3$), 1.44 (s, 18H; C(CH$_3$)$_3$), 1.52–1.73 (br, 24H; CH$_2$ of Cy), 2.06 (s, 24H; PhCH$_3$), 2.16 (s, 24H; PhCH$_3$), 2.21–2.50 (br, 16H; CH$_2$ of Cy), 4.35 (s, 8H; PhCH$_2$O), 6.54 (d, $J = 7.5$ Hz, 8H; PhH), 6.90–7.34 (m, 80H; PhH), 7.43 (t, $J = 7.4$ Hz, 4H; 7,7′-biquino H), 7.71 (t, $J = 7.4$ Hz, 4H; 6,6′-biquino H), 8.03 (d, $J = 8.7$ Hz, 4H; 8,8′-biquino H), 8.22 (d, $J = 1.3$ Hz, 4H; 4,6-isophth H), 8.38 (s, 4H; isophth NH), 8.40 (s, 2H; 2-isophth H), 8.59 (d, $J = 8.7$ Hz, 4H; 5,5′-biquino H), 9.08 (s, 4H; 3,3′-biquino H), 9.41 ppm (s, 4H; biquino NH); ^{13}C NMR (100.6 MHz, [D$_6$]acetone): $\delta =$ 19.2, 19.4, 29.0, 29.3, 29.7, 30.0, 30.3, 31.5, 31.6, 34.8, 114.3, 125.0, 128.9, 131.5, 132.5, 135.6, 137.8, 145.2, 149.3, 164.8, 165.5 ppm; MS (MALDI): m/z: 4563 ([M – PF$_6$]$^+$), 2313 ([M – **17** – PF$_6$]$^+$).

Bis(bipyridyl)-{11′-*tert*-butyl-5′,17′,23′,48′,51′,54′,57′,59′-octamethyldispiro-[cyclohexane-1,2′-{7′,15′,25′,34′,37′,46′-hexaazadecacyclo[45.2.2.2$^{3'.6'}$.2$^{16'.19'}$.2$^{21'.24'}$.1$^{9'.13'}$.1$^{27'.35'}$.1$^{36'.44'}$.0$^{28'.33'}$.0$^{38'.43'}$]hexaconta-3′,5′,9′,11′,13′(58′),16′,18′,21′,23′,27′,29′,31′,33′,35′(53′),36′,38′,40′,42′,44′(52′),47′,49′,50′,54′,56′,59′-pentaeicosaene-8′,14′,26′,45′-tetraone}-20′,1″-cyclohexane]}ruthenium(II) bishexafluorophosphate (22): The (bpy)$_2$Ru^{II} complex of macrocycle **6** was prepared by refluxing **6** (166.8 mg, 0.15 mmol) with an equimolar amount of bipyridine ruthenium dichloride **21** (75.9 mg, 0.15 mmol) in ethylene glycol (15 mL) for 3 h. After the reaction mixture was cooled to 130 °C, part of the solvent was removed by bubbling argon through the solution. After the removal of two-thirds of the solvent, the mixture was cooled to room temperature and dissolved in the minimum volume of water. A clear red solution was formed. Excess NH_4PF_6 was added to this solution and the mixture was stirred at room temperature for 1 h. A red solid was formed, which was collected by filtration, washed thoroughly with water, dried under reduced pressure overnight, and purified by column chromatography on silica. The red fraction with $R_f = 0.6$ (CH_2Cl_2/EtOH, 20/1) was collected. Yield 85%; ^{1}H NMR (500 MHz, [D$_6$]DMSO): $\delta = 1.39$ (s, 9H; C(CH$_3$)$_3$), 1.47 (m, 4H; CH$_2$ of Cy), 1.58 (m, 8H; CH$_2$ of Cy), 2.23 (s, 12H; PhCH$_3$), 2.27 (s, 12H; CH$_2$ of Cy), 2.39 (m, 8H; CH$_2$ of Cy), 6.97 (s, 4H; PhH), 7.13 (s, 4H; PhH), 7.19 (d, $^3J = 8.8$ Hz, 2H; 8,8′-biquino H), 7.38 (dd, $^3J = 8.8$ Hz, $^3J = 8.2$ Hz, 2H; 7,7′-biquino H), 7.52 (t, $^3J = 7.05$, 4H; bipy H), 7.78 (dd, $^3J = 8.2$ Hz, $^3J = 8.4$ Hz, 2H; 6,6′-biquino H), 7.85 (d, $^3J = 5.4$ Hz, 2H; bipy H), 7.91 (d, $^3J = 5.5$ Hz, 2H; bipy H), 8.10 (d, $^4J = 1.1$ Hz, 4,6-isophth H), 8.20 (m, 4H; bipy H), 8.35 (d, $^3J = 8.4$ Hz, 2H; 5,5′-biquino H), 8.61 (s, 1H; 2-isophth H), 8.78 (d, $^3J = 8.5$ Hz, 2H; bipy H), 8.80 (d, $^3J = 8.6$ Hz, 2H; bipy H), 9.01 (s, 2H; 3,3′-biquino H), 9.40 (s, 2H; NH-isophth), 10.31 ppm (s, 2H; NH-biquino); ^{13}C NMR (100.6 MHz, [D$_6$]DMSO): $\delta = 166.0$, 164.8, 161.4, 158.0, 157.7, 154.6, 153.5, 152.7, 152.0, 150.1, 146.9, 145.8, 140.2, 139.8, 136.3, 135.6, 135.6, 133.8, 132.9, 132.4, 131.3, 129.3, 128.7, 128.1, 128.0, 127.6, 126.6, 126.2, 126.0, 126.0, 125.2, 123.1, 120.4, 49.0, 45.7, 35.2, 31.4, 23.2, 20.7, 19.4, 19.1 ppm; MS (MALDI): m/z: 1697.5 ([M – PF$_6$]$^+$, 15%), 1552.4 ([M – 2PF$_6$]$^+$, 100%).

Crystal structure determination of building block 4: Single crystals suitable for X-ray diffraction experiments were obtained by recrystallization of **4** from DMSO. The structure was solved by direct methods (SHELXS-97).[43] The non-hydrogen atoms were refined anisotropically against F^2 (SHELXL-97).[44] H atoms were refined using a riding model. Two DMSO solvent molecules were found to be highly disordered. Further details are given in Table 1. A detailed description of the crystal structure can be found in the Supporting Information accompanying this paper. CCDC-193229 contains the supplementary crystallographic data for this paper. These data can be obtained free of charge via www.ccdc.cam.ac.uk/conts/retrieving.html (or from the Cambridge Crystallographic Data Centre, 12, Union Road, Cambridge CB2 1EZ, UK; fax: (+44) 1223-336-033; or deposit@ccdc.cam.ac.uk).

^{1}H NMR titrations: First, a Job plot analysis was carried out in [D$_6$]DMSO with the hosts and tetrabutylammonium salt of the guest to confirm a 1:1 stoichiometry for the complexes observed. In order to determine the binding constants for chloride, 4mM solutions of the free macrocycle and the corresponding (bpy)$_2$Ru(II) complex were each titrated separately in [D$_6$]DMSO with up to 16 equivalents of tetrabutylammonium chloride as the guest salt, and the shifts of the proton signals were monitored as described in the text. The titration curves were fitted with the global analysis program Specfit 3.0.31 for Windows.[45] For dihydrogen phosphate, good fits were obtained with a simple model including the free receptors, the anion, and the 1:1 complex as the species present in solution. For the halide, the fit was further improved if a 1:2 complex of receptor and chloride was also taken into account. There is no aggregation of the receptors in DMSO and thus this was not considered in the model.

Molecular modeling: Building block **4**, the macrocycles **6** and **8**, and the catenane **7** were examined with the Amber* force field[24] as implemented in the MacroModel 7.1 program package.[25] In our experience, this method gives excellent results, especially when noncovalent interactions such as hydrogen-bonding and van der Waals forces are operative. We were interested in the lowest energy conformations, in particular with respect to the dihedral angle between the two aromatic planes in each biquinoline moiety. The lowest energy conformers out of 3000 structures were determined using the Monte Carlo algorithm provided with this program. Closure bonds were placed in the macrocycles (one of the amide bonds) and the attached cyclohexyl side chains. While the aromatic rings and the amides were constrained to planarity, all single bonds (with the exception of the methyl groups) were given the freedom to allow rotations into other conformations. Finally, the two wheels of catenane **7** were treated as independent molecules which could move relative to each other. It should be noted that during the search, the catenane may convert to a structure consisting of two independent macrocycles. This problem is merely due to the algorithm, which treats cyclic molecules like chains by opening one covalent bond (the closure bond). This does not, of course, have any chemical implications. To prevent the problem, it is wise to choose amide bonds at the periphery as closure bonds with a maximum closure distance of 2 Å. For each minimization, the number of iterations was set to 10000 in order to generate fully converged structures. The energy range for

structures to store in the output file was set at 100 kJ mol^{-1} above the lowest energy conformer.

For the copper and ruthenium complexes, the MacroModel program does not provide the necessary parameters for modeling the metal-centered cores of the molecules. We therefore used the augmented MM2 force field as implemented in the CACHE 5.0 program package for these complexes. After minimization of a local minimum, several dynamics calculations were performed for 1000 ps at 600 K with a step size of 2 fs. The energetically most favorable conformers were then reoptimized with the MM2 force field.

Acknowledgements

We are grateful to Prof. Fritz Vögtle for valuable suggestions and inspiring discussions. We thank Gabriele Silva for help with the synthesis. Dr. Jörg Hörnschemeyer is acknowledged for technical assistance with ESI-MS experiments. X.-y.L. thanks the Alexander von Humboldt foundation for a postdoctoral research fellowship. C.A.S. acknowledges support by the Fonds der Chemischen Industrie (Liebig research fellowship), and the Deutsche Forschungsgemeinschaft for funding this project.

[1] For reviews on mechanically interlocked molecules, see: a) G. Schill, *Catenanes, Rotaxanes and Knots*, Academic Press, New York, **1971**; b) C. O. Dietrich-Buchecker, J.-P. Sauvage, *Chem. Rev.* **1987**, *87*, 795; c) J.-P. Sauvage, *Acc. Chem. Res.* **1990**, *23*, 319; d) S. Anderson, H. L. Anderson, J. K. M. Sanders, *Acc. Chem. Res.* **1993**, *26*, 469; e) R. Hoss, F. Vögtle, *Angew. Chem.* **1994**, *106*, 389; *Angew. Chem. Int. Ed. Engl.* **1994**, *33*, 375; f) D. A. Amabilino, J. F. Stoddart, *Chem. Rev.* **1995**, *95*, 2725; g) J.-C. Chambron, C. O. Dietrich-Buchecker, V. Heitz, J.-F. Nierengarten, J.-P. Sauvage, C. Pascard, J. Guilhem, *Pure Appl. Chem.* **1995**, *67*, 233; h) R. Jäger, F. Vögtle, *Angew. Chem.* **1997**, *109*, 966; *Angew. Chem. Int. Ed. Engl.* **1997**, *36*, 931; i) S. A. Nepogodiev, J. F. Stoddart, *Chem. Rev.* **1998**, *98*, 1959; j) F. M. Raymo, J. F. Stoddart, *Chem. Rev.* **1999**, *99*, 1043; k) *Molecular Catenanes, Rotaxanes, and Knots*, (Eds.: J.-P. Sauvage, C. Dietrich-Buchecker), Wiley-VCH, Weinheim, **1999**.

[2] Reviews on template effects in general: a) D. H. Busch, N. A. Stephensen, *Coord. Chem. Rev.* **1990**, *90*, 119; b) R. Cacciapaglia, L. Mandolini, *Chem. Soc. Rev.* **1993**, *22*, 221; c) N. V. Gerbeleu, V. B. Arion, J. Burgess, *Template Synthesis of Macrocyclic Compounds*, Wiley-VCH, Weinheim, **1999**; d) *Templated Organic Synthesis*, (Eds.: F. Diederich, P. J. Stang) Wiley-VCH, Weinheim, **2000**; e) T. J. Hubin, D. H. Busch, *Coord. Chem. Rev.* **2000**, *100*, 5.

[3] Selected examples: a) C. O. Dietrich-Buchecker, J.-P. Sauvage, J.-P. Kintzinger, *Tetrahedron Lett.* **1983**, *24*, 5095; b) A. M. A. Gary, C. O. Dietrich-Buchecker, Z. Saad, J.-P. Sauvage, *J. Am. Chem. Soc.* **1988**, *110*, 1467; c) A. Livoreil, C. O. Dietrich-Buchecker, J.-P. Sauvage, *J. Am. Chem. Soc.* **1994**, *116*, 9399; d) F. Baumann, A. Livoreil, W. Kaim, J.-P. Sauvage, *Chem. Commun.* **1997**, 35; e) A. Livoreil, J.-P. Sauvage, N. Amaroli, V. Balzani, L. Flamigni, B. Ventura, *J. Am. Chem. Soc.* **1997**, *119*, 12114; f) J.-C. Chambron, J.-P. Sauvage, K. Mislow, A. De Cian, J. Fischer, *Chem. Eur. J.* **2001**, *7*, 4085.

[4] D. A. Leigh, P. J. Lusby, S. J. Teat, A. J. Wilson, J. K. Y. Wong, *Angew. Chem.* **2001**, *113*, 1586; *Angew. Chem. Int. Ed.* **2001**, *40*, 1538.

[5] For selected examples, see: a) B. L. Allwood, N. Spencer, H. Shahriari-Zavareh, J. F. Stoddart, D. J. Williams, *J. Chem. Soc. Chem. Commun.* **1987**, 1064; b) P. R. Ashton, I. Iriepa, M. V. Reddington, N. Spencer, A. M. Z. Slawin, J. F. Stoddart, D. J. Williams, *Tetrahedron Lett.* **1994**, *35*, 4835; c) M. Asakawa, P. R. Ashton, S. E. Boyd, C. L. Brown, S. Menzer, S. Pasini, J. F. Stoddart, M. S. Tolley, A. J. P. White, D. J. Williams, P. G. Wyatt, *Chem. Eur. J.* **1997**, *3*, 463.

[6] For examples, see: a) A. G. Kolchinski, D. H. Busch, N. W. Alcock, *J. Chem. Soc. Chem. Commun.* **1995**, 1289; b) P. T. Glink, C. Schiavo, J. F. Stoddart, D. J. Williams, *J. Chem. Soc. Chem. Commun.* **1996**, 1483; c) P. R. Ashton, A. N. Collins, M. C. T. Fyfe, S. Menzer, J. F. Stoddart, D. J. Williams, *Angew. Chem.* **1997**, *109*, 760; *Angew. Chem. Int. Ed.* **1997**, *36*, 735; d) F. G. Gatti, D. A. Leigh, S. A. Nepogodiev, A. M. Z. Slawin, S. J. Teat, J. K. Y. Wong, *J. Am. Chem. Soc.* **2001**, *123*, 5983.

[7] For a few examples, see: a) H. Adams, F. J. Carver, C. A. Hunter, *J. Chem. Soc. Chem. Commun.* **1995**, 809; b) A. G. Johnston, D. A. Leigh, R. J. Pritchard, M. D. Deegan, *Angew. Chem.* **1995**, *107*, 1324; *Angew. Chem. Int. Ed.* **1995**, *34*, 1209; c) Y. Geerts, D. Muscat, K. Müllen, *Macromol. Chem. Phys.* **1995**, *196*, 3425; d) T. Dünnwald, A. H. Parham, F. Vögtle, *Synthesis* **1998**, *3*, 339; e) O. Safarowsky, E. Vogel, F. Vögtle, *Eur. J. Org. Chem.* **2000**, 499.

[8] a) G. M. Hübner, J. Gläser, C. Seel, F. Vögtle, *Angew. Chem.* **1999**, *111*, 395; *Angew. Chem. Int. Ed.* **1999**, *38*, 383; b) C. Reuter, W. Wienand, G. M. Hübner, C. Seel, F. Vögtle, *Chem. Eur. J.* **1999**, *5*, 2692; c) C. Seel, F. Vögtle, *Chem. Eur. J.* **2000**, *6*, 21; d) C. A. Schalley, G. Silva, C. F. Nising, P. Linnartz, *Helv. Chim. Acta* **2002**, *85*, 1578; e) P. Ghosh, O. Mermagen, C. A. Schalley, *Chem. Commun.* **2002**, 2628.

[9] a) D. K. Mitchell, J.-P. Sauvage, *Angew. Chem.* **1988**, *100*, 985; *Angew. Chem. Int. Ed. Engl.* **1988**, *27*, 930; b) Y. Kaida, Y. Okamoto, J.-C. Chambron, D. K. Mitchell, J.-P. Sauvage, *Tetrahedron Lett.* **1993**, *34*, 1019; c) P. R. Ashton, A. S. Reder, N. Spencer, J. F. Stoddart, *J. Am. Chem. Soc.* **1993**, *115*, 5286; d) C. Yamamoto, Y. Okamoto, T. Schmidt, R. Jäger, F. Vögtle, *J. Am. Chem. Soc.* **1997**, *119*, 10547; e) P. R. Ashton, J. A. Bravo, F. M. Raymo, J. F. Stoddart, A. J. P. White, D. J. Williams, *Eur. J. Org. Chem.* **1999**, 899; f) R. Schmieder, G. Hübner, C. Seel, F. Vögtle, *Angew. Chem.* **1999**, *111*, 3741; *Angew. Chem. Int. Ed.* **1999**, *38*, 3528; g) C. Reuter, A. Mohry, A. Sobanski, F. Vögtle, *Chem. Eur. J.* **2000**, *6*, 1674. For a review, see: h) J.-C. Chambron, C. O. Dietrich-Buchecker, J.-P. Sauvage, *Top. Curr. Chem.* **1993**, *165*, 131.

[10] a) D. J. Cárdenas, P. Gaviñas, J.-P. Sauvage, *Chem. Commun.* **1996**, 1915; b) D. B. Amabilino, C. O. Dietrich-Buchecker, J.-P. Sauvage, *J. Am. Chem. Soc.* **1996**, *118*, 3285; c) D. J. Cárdenas, P. Gaviñas, J.-P. Sauvage, *J. Am. Chem. Soc.* **1997**, *119*, 2656. For a review, see: d) J.-C. Chambron, S. Chardon-Noblat, A. Harriman, V. Heitz, J.-P. Sauvage, *Pure Appl. Chem.* **1993**, *65*, 2343.

[11] F. Diederich, L. Echegoyen, M. Gómez-López, R. Kessinger, J. F. Stoddart, *J. Chem. Soc. Perkin Trans. 2* **1999**, 1577.

[12] F. Vögtle, W. M. Müller, U. Müller, M. Bauer, K. Rissanen, *Angew. Chem.* **1993**, *105*, 1356; *Angew. Chem. Int. Ed. Engl.* **1993**, *32*, 1295.

[13] S. S. Zhu, P. J. Carroll, T. M. Swager, *J. Am. Chem. Soc.* **1996**, *118*, 8713.

[14] a) F. M. Raymo, K. N. Houk, J. F. Stoddart, *J. Am. Chem. Soc.* **1998**, *120*, 9318; b) A. Affeld, G. M. Hübner, C. Seel, C. A. Schalley, *Eur. J. Org. Chem.* **2001**, 2877, and references therein.

[15] a) A. Credi, V. Balzani, S. J. Langford, J. F. Stoddart, *J. Am. Chem. Soc.* **1997**, *119*, 2679; b) M. Asakawa, P. R. Ashton, V. Balzani, A. Credi, G. Mattersteig, O. A. Matthews, M. Montalti, N. Spencer, J. F. Stoddart, M. Venturi, *Chem. Eur. J.* **1997**, *3*, 1992.

[16] a) K. E. Drexler, *Annu. Rev. Biophys. Biomol. Struct.* **1994**, *23*, 377; b) V. Balzani, M. Gómez-López, J. F. Stoddart, *Acc. Chem. Res.* **1998**, *31*, 405; c) J.-P. Sauvage, *Acc. Chem. Res.* **1998**, *31*, 611; d) J.-P. Collin, P. Gaviña, V. Heitz, J.-P. Sauvage, *Eur. J. Inorg. Chem.* **1998**, 1; e) Z. Asfari, J. Vicens, *J. Incl. Phenom. Macrocycl. Chem.* **2000**, *36*, 103; f) V. Balzani, A. Credi, F. M. Raymo, J. F. Stoddart, *Angew. Chem.* **2000**, *112*, 3484; *Angew. Chem. Int. Ed.* **2000**, *39*, 3348; g) C. A. Schalley, K. Beizai, F. Vögtle, *Acc. Chem. Res.* **2001**, *34*, 465; h) J.-P. Collin, C. Dietrich-Buchecker, P. Gaviña, M. C. Jimenez-Molero, J.-P. Sauvage, *Acc. Chem. Res.* **2001**, *34*, 477; i) A. W. Shipway, I. Willner, *Acc. Chem. Res.* **2001**, *34*, 421; j) A. R. Pease, J. O. Jeppesen, J. F. Stoddart, Y. Luo, C. P. Collier, J. R. Heath, *Acc. Chem. Res.* **2001**, *34*, 433; k) R. Ballardini, V. Balzani, A. Credi, M. T. Gandolfei, M. Venturi, *Acc. Chem. Res.* **2001**, *34*, 445.

[17] Y. Lei, F. C. Anson, *Inorg. Chem.* **1995**, *34*, 1083.

[18] a) D. S. Sigman, T. W. Bruice, A. Mazumder, C. L. Sutton, *Acc. Chem. Res.* **1993**, *26*, 98; b) M. M. Meijie, O. Zelenko, D. S. Sigman, *J. Am. Chem. Soc.* **1997**, *119*, 1135, and references therein.

[19] a) F. N. Castellano, M. Ruthkosky, G. J. Meyer, *Inorg. Chem.* **1995**, *34*, 3; b) M. Ruthkosky, F. N. Castellano, G. J. Meyer, *Inorg. Chem.* **1996**, *35*, 6404.

[20] For recent reviews, see: a) C. Seel, A. Galán, J. de Mendoza, *Top. Curr. Chem.* **1995**, *175*, 101; b) F. P. Schmidtchen, M. Berger, *Chem. Rev.* **1997**, *97*, 1609; c) P. D. Beer, *Acc. Chem. Res.* **1998**, *31*, 71; d) P. Bühlmann, E. Pretsch, E. Bakker, *Chem. Rev.* **1998**, *98*, 1593; e) P. A. Gale, J. L. Sessler, V. Král, *Chem. Commun.* **1998**, 1; f) P. D. Beer, P. A. Gale, *Angew. Chem.* **2001**, *113*, 502; *Angew. Chem. Int. Ed.* **2001**, *40*, 487; g) J. J. Lavigne, E. V. Anslyn, *Angew. Chem.* **2001**, *113*, 3212;

  0947-6539/03/0906-1346 $ 20.00+.50/0

Angew. Chem. Int. Ed. **2001**, *40*, 3119; h) P. A. Gale, P. Anzenbacher, Jr., J. L. Sessler, *Coord. Chem. Rev.* **2001**, *101*, 57; i) J. L. Sessler, J. M. Davis, *Acc. Chem. Res.* **2001**, *34*, 989; j) P. A. Gale, *Coord. Chem. Rev.* **2001**, *101*, 79; k) J. J. Bodwin, A. D. Cutland, R. G. Malkani, V. L. Pecoraro, *Coord. Chem. Rev.* **2001**, *101*, 489; l) V. Amendola, L. Fabrizzi, C. Mangano, P. Pallavicini, A. Poggi, A. Taglietti, *Coord. Chem. Rev.* **2001**, *101*, 821.

[21] For a selection of general reviews on self-assembly, see: a) G. M. Whitesides, J. P. Mathias, C. T. Seto, *Science* **1991**, *254*, 1312; b) D. Philp, J. F. Stoddart, *Angew. Chem.* **1996**, *108*, 1242; *Angew. Chem. Int. Ed. Engl.* **1996**, *35*, 1154; c) C. Piguet, G. Bernardinelli, G. Hopfgartner, *Chem. Rev.* **1997**, *97*, 2005; d) M. Albrecht, *Chem. Soc. Rev.* **1998**, *27*, 281; e) C. J. Jones, *Chem. Soc. Rev.* **1998**, *27*, 289; f) C. Piguet, *J. Inclusion Phenom. Macrocycl. Chem.* **1999**, *34*, 361; g) J.-M. Lehn, *Chem. Eur. J.* **2000**, *6*, 2097; h) M. Fujita, K. Umemoto, M. Yoshizawa, N. Fujita, T. Kusukawa, K. Biradha, *Chem. Commun.* **2001**, 509; i) G. F. Swiegers, T. J. Malfetse, *J. Inclusion Phenom. Macrocycl. Chem.* **2001**, *40*, 253; j) M. Albrecht, *Chem. Rev.* **2001**, *101*, 3457.

[22] a) O. Waldmann, J. Hassmann, P. Müller, G. S. Hanan, D. Volkmer, U. S. Schubert, J.-M. Lehn, *Phys. Rev. Lett.* **1997**, *78*, 3390; b) A. Semenov, J. P. Spatz, M. Möller, J.-M. Lehn, B. Sell, D. Schubert, C. H. Weidl, U. S. Schubert, *Angew. Chem.* **1999**, *111*, 2701; *Angew. Chem. Int. Ed.* **1999**, *38*, 2547; c) J. Rojo, F. J. Romero-Salguero, J.-M. Lehn, G. Baum, D. Fenske, *Eur. J. Inorg. Chem.* **1999**, 1421; d) P. N. W. Baxter, J.-M. Lehn, G. Baum, D. Fenske, *Chem. Eur. J.* **2000**, *6*, 4510; e) D. P. Funeriu, J.-M. Lehn, K. M. Fromm, D. Fenske, *Chem. Eur. J.* **2000**, *6*, 2103; f) P. N. W. Baxter, R. G. Khoury, J.-M. Lehn, G. Baum, D. Fenske, *Chem. Eur. J.* **2000**, *6*, 4140; g) E. Breuning, U. Ziener, J.-M. Lehn, E. Wegelius, K. Rissanen, *Eur. J. Inorg. Chem.* **2001**, 1515; h) T. Bark, M. Düggeli, H. Stoeckli-Evans, A. von Zelewsky, *Angew. Chem.* **2001**, *113*, 2924; *Angew. Chem. Int. Ed.* **2001**, *40*, 2848; i) O. Mamula, F. J. Monlien, A. Porquet, G. Hopfgartner, A. E. Merbach, A. von Zelewsky, *Chem. Eur. J.* **2001**, *7*, 533; j) M. Schmittel, C. Michel, A. Wiegrefe, V. Kalsani, *Synthesis* **2001**, 1561; k) U. Ziener, J.-M. Lehn, A. Mourran, M. Möller, *Chem. Eur. J.* **2002**, *8*, 951; l) A. Lützen, M. Hapke, J. Griep-Raming, D. Haase, W. Saak, *Angew. Chem.* **2002**, *114*, 2190; *Angew. Chem. Int. Ed.* **2001**, *41*, 2086.

[23] a) C. A. Hunter, *J. Chem. Soc. Chem. Commun.* **1991**, 749; b) C. A. Hunter, *J. Am. Chem. Soc.* **1992**, *114*, 5303; c) C. A. Hunter, D. H. Purvis, *Angew. Chem.* **1992**, *104*, 779; *Angew. Chem. Int. Ed. Engl.* **1992**, *31*, 792; d) S. Ottens-Hildebrandt, T. Schmidt, J. Harren, F. Vögtle, *Liebigs Ann.* **1995**, 1855; e) R. Jäger, M. Händel, K. Rissanen, F. Vögtle, *Liebigs Ann.* **1996**, 1201; f) F. Vögtle, R. Jäger, M. Händel, S. Ottens-Hildebrandt, W. Schmidt, *Synthesis* **1996**, 353.

[24] a) S. J. Weiner, P. A. Kollman, D. A. Case, U. C. Singh, G. Alagona, S. Profeta, P. Weiner, *J. Am. Chem. Soc.* **1984**, *106*, 765; b) S. J. Weiner, P. A. Kollman, N. T. Nguyen, D. A. Case, *J. Comput. Chem.* **1987**, *7*, 230; c) D. M. Ferguson, P. A. Kollman, *J. Comput. Chem.* **1991**, *12*, 620.

[25] Schrödinger, Inc. 1500 SW First Avenue, Suite 1180, Portland, OR 97201, USA. Also, see: a) F. Mohamadi, N. G. Richards, W. C. Guida, R. Liskamp, C. Caulfield, G. Chang, T. Hendrickson, W. C. Still, *J. Comput. Chem.* **1990**, *11*, 440; b) D. Q. McDonald, W. C. Still, *Tetrahedron Lett.* **1992**, *33*, 7743.

[26] Several of these DMSO molecules are disordered and this disorder is responsible for the rather high *R* value (Table 1). Nevertheless, the structure is of sufficient quality to deduce the transoid conformation of the biquinoline moiety of **4**.

[27] a) C. Reuter, C. Seel, M. Nieger, F. Vögtle, *Helv. Chim. Acta* **2000**, *83*, 630; b) A. Mohry, F. Vögtle, M. Nieger, H. Hupfer, *Chirality* **2000**, *12*, 76.

[28] C. Seel, A. H. Parham, O. Safarowsky, G. M. Hübner, F. Vögtle, *J. Org. Chem.* **1999**, *64*, 7236.

[29] P. Belser, A. von Zelewsky, *Helv. Chim. Acta* **1980**, *63*, 1675.

[30] CACHE 5.0 for Windows, Fujitsu Ltd. **2001**, Krakow, Poland.

[31] a) R. P. Thummel, F. Lefoulon, *Inorg. Chem.* **1987**, *26*, 675; b) D. P. Funeriu, J.-M. Lehn, G. Baum, D. Fenske, *Chem. Eur. J.* **1997**, *3*, 99.

[32] a) V. Goulle, R. P. Thummel, *Inorg. Chem.* **1990**, *29*, 1767; b) Y. Jahng, J. Hazelrigg, D. Kimball, E. Riesgo, F. Wu, R. P. Thummel, *Inorg. Chem.* **1997**, *36*, 5390; c) M. Schmittel, C. Michel, S.-X. Liu, D. Schildbach, D. Fenske, *Eur. J. Inorg. Chem.* **2001**, 1155.

[33] C. A. Schalley, J. Hörnschemeyer, X.-y. Li, G. Silva, P. Weis, *Int. J. Mass, Spectrom*. in press.

[34] Similar findings have been reported before. See, for example: P. R. Ashton, V. Baldoni, V. Balzani, A. Credi, H. D. A. Hoffmann, M.-V. Martínez-Díaz, F. M. Raymo, J. F. Stoddart, M. Venturi, *Chem. Eur. J.* **2001**, *7*, 3482.

[35] For recent reviews on the mass spectrometry of supramolecular entities, see: a) C. A. Schalley, *Int. J. Mass Spectrom.* **2000**, *194*, 11; b) C. A. Schalley, *Mass Spectrom. Rev.* **2001**, *20*, 253. See also: c) C. A. Schalley, T. Müller, P. Linnartz, M. Witt, M. Schäfer, A. Lützen, *Chem. Eur. J.* **2002**, *8*, 3538.

[36] For reviews on anion binding, see, for example: reference [20].

[37] a) D. H. Vance, A. W. Czarnik, *J. Am. Chem. Soc.* **1994**, *116*, 9397; b) P. D. Beer, *Chem. Commun.* **1996**, 689; c) A. P. de Silva, H. Q. N. Gunaratine, C. McVergh, G. E. M. Maguire, P. R. S. Maxwell, E. O'Hanlon, *Chem. Commun.* **1996**, 2191; d) A. Andrievsky, F. Ahuis, J. L. Sessler, F. Vögtle, D. Gudat, M. Moini, *J. Am. Chem. Soc.* **1998**, *120*, 9712; e) K. Kavallieratos, C. M. Bertao, R. H. Crabtree, *J. Org. Chem.* **1999**, *64*, 1675; f) A. Szumna, J. Jurczak, *Eur. J. Org. Chem.* **2001**, 4031; g) A. J. Ayling, S. Broderick, J. P. Clare, A. P. Davis, M. N. Pérez-Payán, M. Lahtinen, M. J. Nissinen, K. Rissanen, *Chem. Eur. J.* **2002**, *8*, 2197.

[38] a) P. D. Beer, F. Szemes, V. Balzani, C. M. Salà, M. G. B. Drew, S. W. Dent, M. Maestri, *J. Am. Chem. Soc.* **1997**, *119*, 11864; b) S. Watanabe, O. Onogawa, Y. Komatsu, K. Yoshida, *J. Am. Chem. Soc.* **1998**, *120*, 229; c) V. W.-W. Yam, A. S.-F. Kai, *Chem. Commun.* **1998**, 109; d) P. D. Beer, V. Timoshenko, M. Maestri, P. Passaniti, V. Balzani, *Chem. Commun.* **1999**, 1755; e) P. D. Beer, J. Cadman, *New J. Chem.* **1999**, *23*, 347; f) T. Mizuno, W.-H. Wei, L. R. Eller, J. L. Sessler, *J. Am. Chem. Soc.* **2002**, *124*, 1134; g) P. Anzenbacher, Jr., D. S. Tyson, K. Jursíková, F. N. Castellano, *J. Am. Chem. Soc.* **2002**, *124*, 6232.

[39] K. A. Connors, *Binding Constants*, Wiley, New York, **1987**.

[40] a) M. Schmittel, A. Ganz, *Synlett* **1997**, 710; b) M. Schmittel, A. Ganz, *Chem. Commun.* **1997**, 999; c) M. Schmittel, H. Ammon, *Synlett* **1999**, 750; d) M. Schmittel, C. Michel, A. Ganz, M. Herderich, *J. Prakt. Chem. - Chem. Ztg.* **1999**, *341*, 228; f) M. Schmittel, A. Ganz, D. Fenske, *Org. Lett.* **2002**, *4*, 2289.

[41] A. S. Hünten, *Ph. D. Thesis*, Universität Bonn, **2000**.

[42] H. W. Gibson, S. H. Lee, P. T. Engen, P. Lecavalier, J. Sze, X. Y. Shen, M. J. Bheda, *Org. Chem.* **1993**, 58, 3748.

[43] G. M. Sheldrick, SHELXS-90, *Acta Crystallogr. Sect. A* **1990**, *46*, 467.

[44] G. M. Sheldrick, SHELXL-97, Universität Göttingen, Germany, **1997**.

[45] Spectrum Software Associates, Chapel Hill, NC, USA; H. Gampp, M. Maeder, C. J. Meyer, A. D. Zuberbühler, *Talanta* **1986**, *33*, 943, and references therein.

Received: September 12, 2002 [F4419]